Precise Orbit Determination (POD)
of Low Earth Orbiters (LEOs)
using the Global Positioning System (GPS)

Adrian Jäggi

Astronomical Institute
University of Bern

Low Earth Orbiters (LEOs)

CHAMP

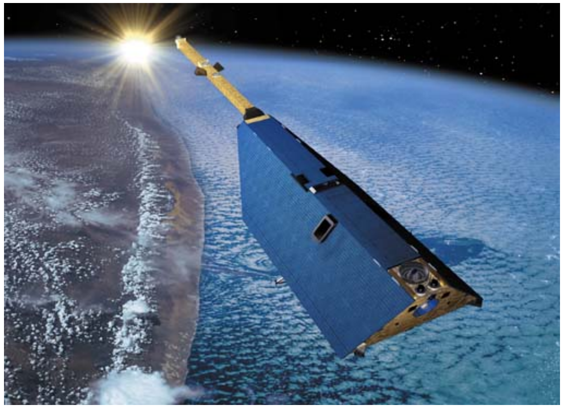

CHA**llenging** **M**inisatellite **P**ayload

GRACE

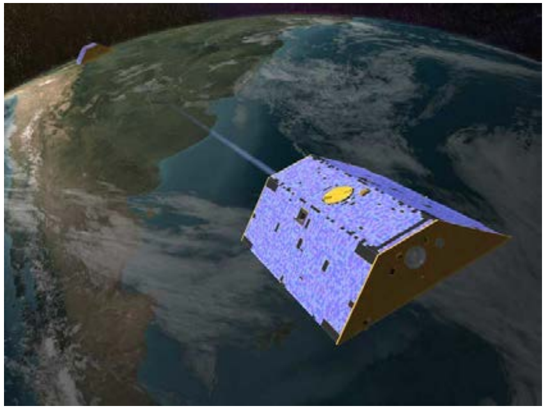

Gravity **R**ecovery **A**nd **C**limate **E**xperiment

GOCE

Gravity and steady-state **O**cean **C**irculation **E**xplorer

But there are many more missions equipped with GPS receivers …

Jason

Jason-2

MetOp-A

Icesat

COSMIC

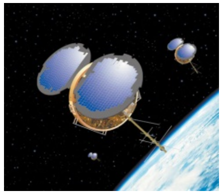

LEO Constellations

TanDEM-X

Swarm

Sentinel

and of course, in the near future

LEO Precise Orbit Determination (POD)

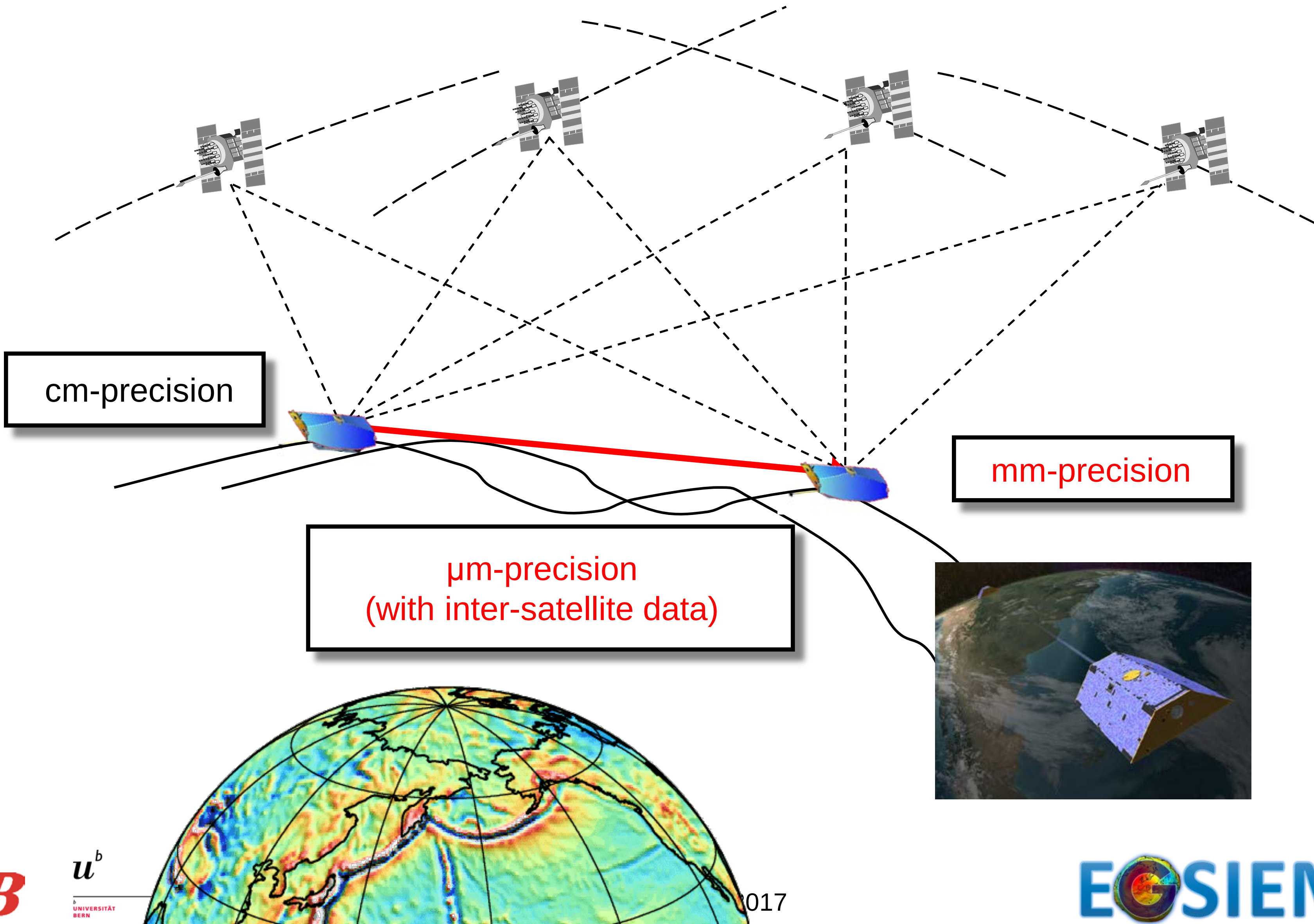

Global Navigation Satellite Systems (GNSS)

GPS

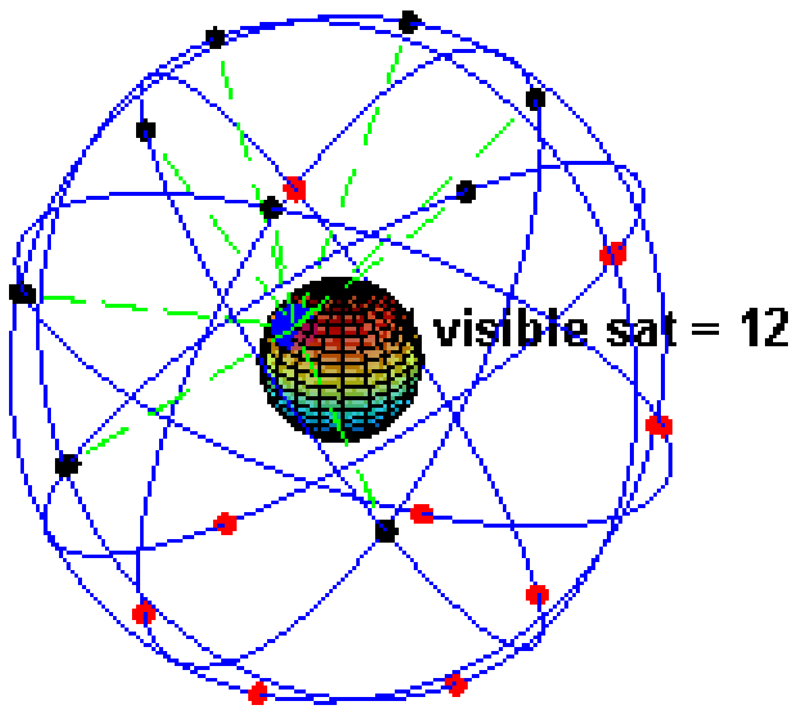

Galileo

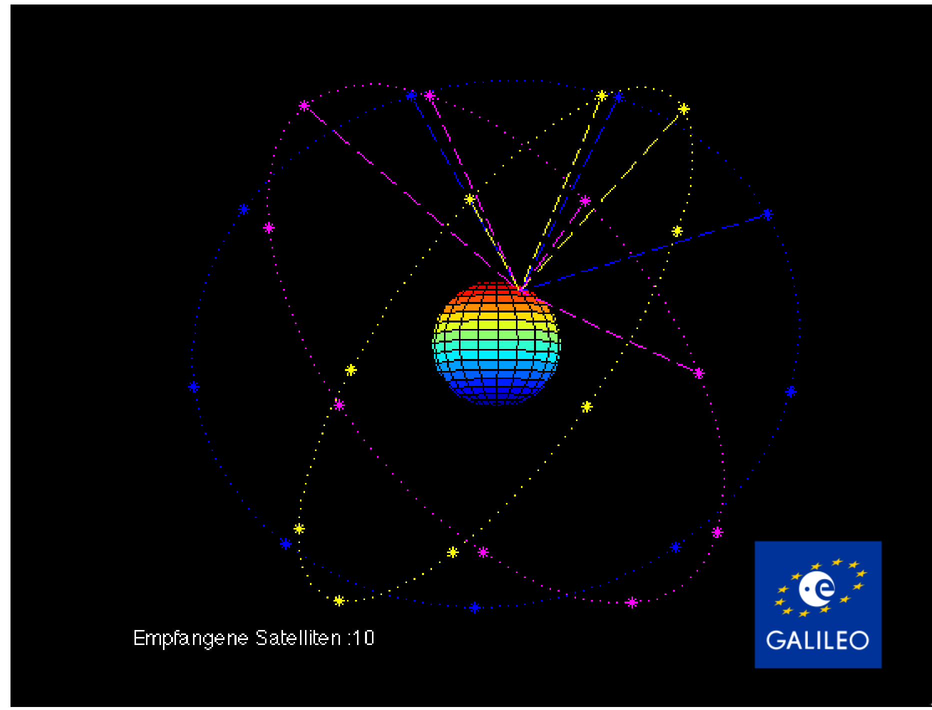

Other GNSS are already existing (GLONASS) or being built up (Galileo, Beidou), but there are no multi-GNSS spaceborne receivers (with open data policy) in LEO orbit yet.

Introduction to GPS

GPS: **G**lobal **P**ositioning **S**ystem

Characteristics:

- Satellite system for (real-time) **Positioning** and **Navigation**
- **Global** (everywhere on Earth, up to altitudes of 5000km) and **at any time**
- **Unlimited** number of users
- **Weather-independent** (radio signals are passing through the atmosphere)
- **3-dimensional position**, **velocity** and **time** information

Global Network of the International GNSS Service (IGS)

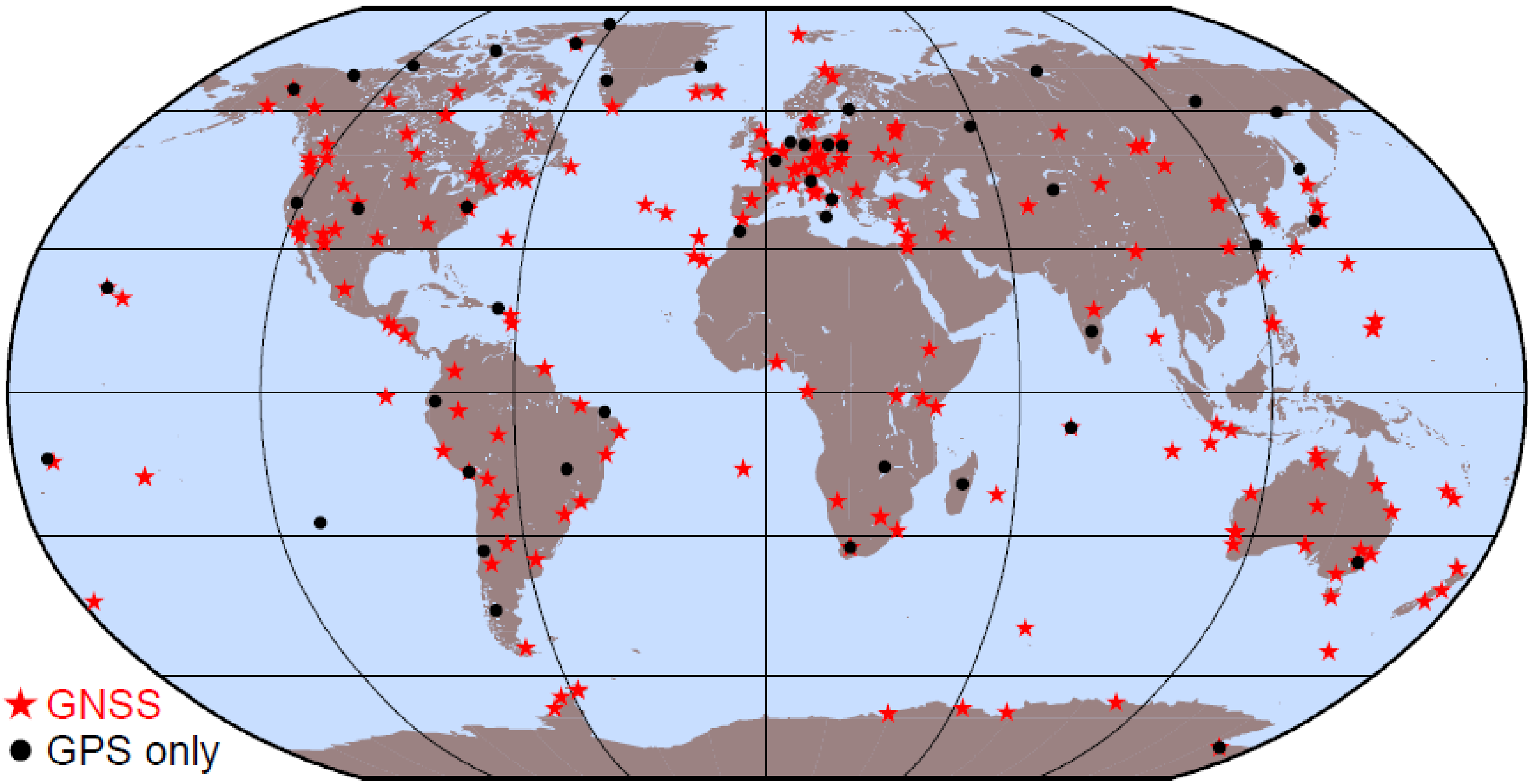

IGS stations used for computation of final orbits at UBERN (CODE) in June 2016 (Dach et al., 2009)

Parameters of a Global IGS Solution

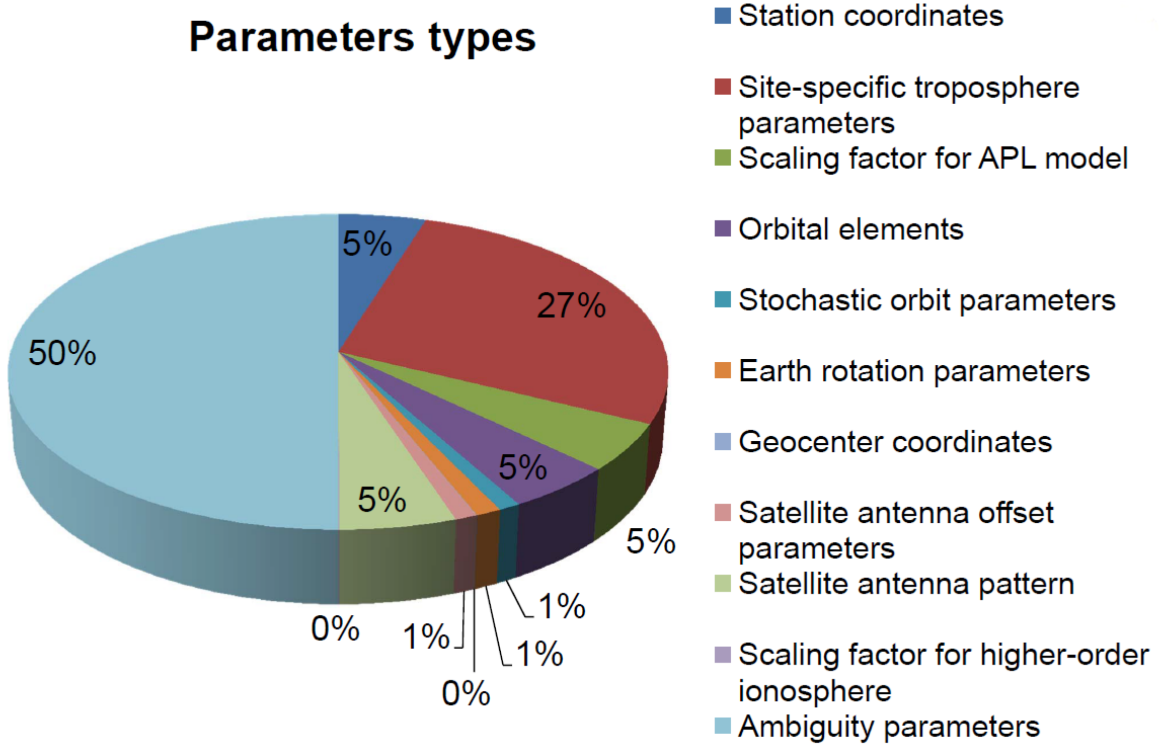

- A large parameter estimation problem needs to be solved to determine GPS satellite orbits together with many other parameters on a routine basis
- Thanks to this continuous effort performed by the Analysis Centers (ACs) of the **International GNSS Service (IGS)** many scientific applications are enabled

Performance of IGS Final Orbits

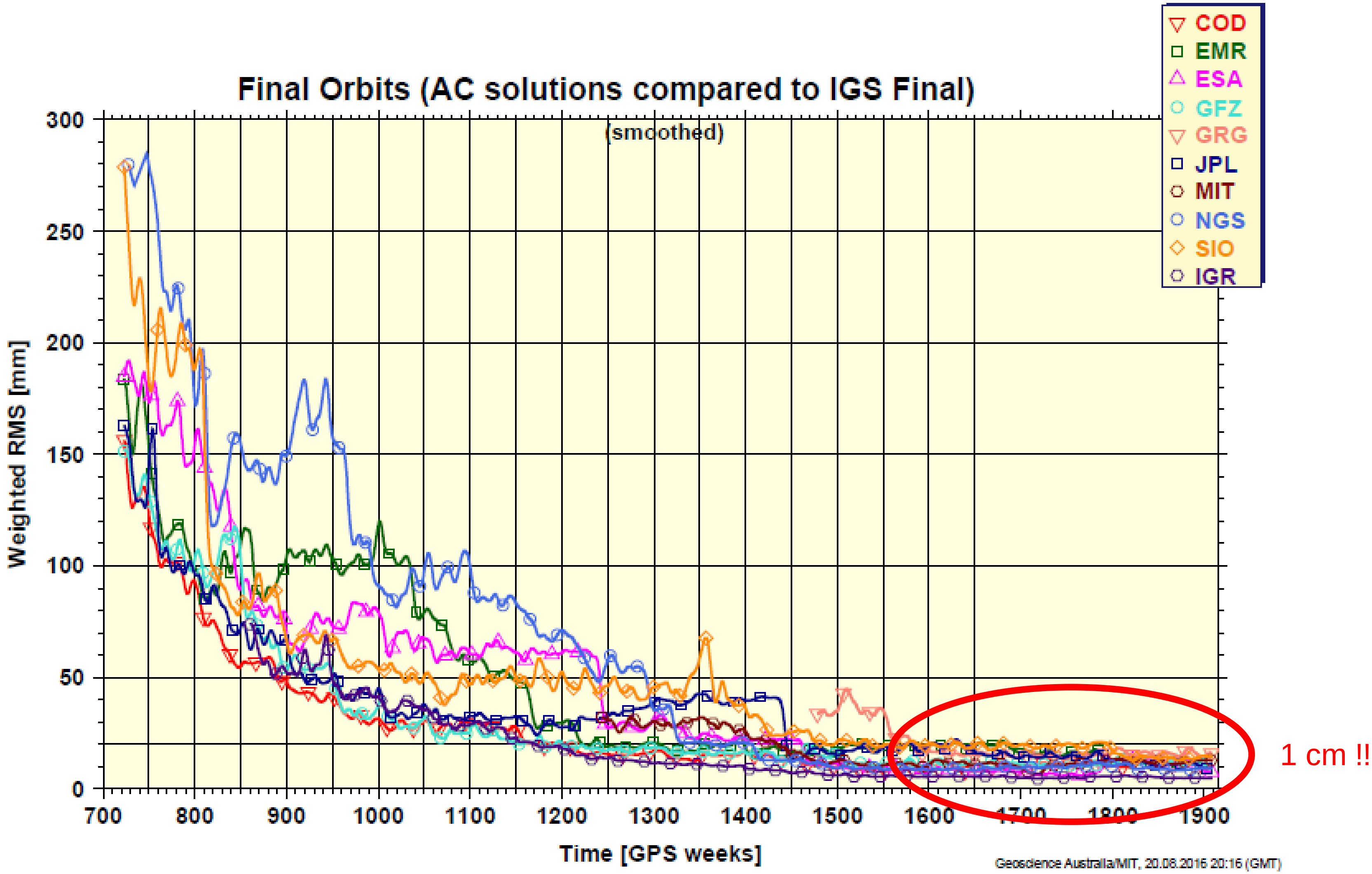

GNSS Solar Radiation Pressure Modeling

Old Extended CODE Orbit Model (ECOM) was represented by

$$\mathbf{a} = \mathbf{a}_0 + D(u)\mathbf{e}_D + Y(u)\mathbf{e}_Y + B(u)\mathbf{e}_B$$

with $\mathbf{e}_D \doteq \dfrac{\mathbf{r}_s - \mathbf{r}}{|\mathbf{r}_s - \mathbf{r}|}, \ \mathbf{e}_Y \doteq -\dfrac{\mathbf{e}_r \times \mathbf{e}_D}{|\mathbf{e}_r \times \mathbf{e}_D|}, \ \mathbf{e}_B \doteq \mathbf{e}_D \times \mathbf{e}_Y$,

and

$$D(u) = D_0 + D_c \cos u + D_s \sin u$$
$$Y(u) = Y_0 + Y_c \cos u + Y_s \sin u$$
$$B(u) = B_0 + B_c \cos u + B_s \sin u$$

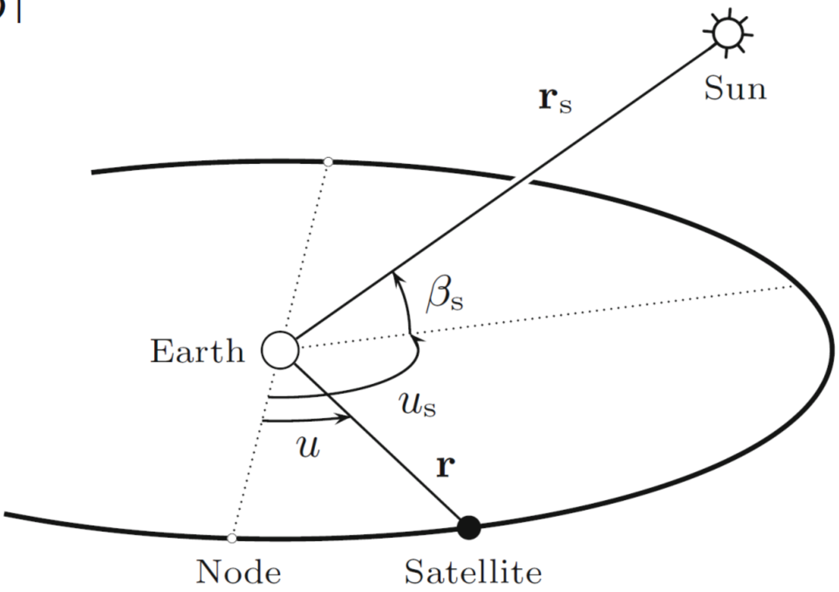

GNSS Solar Radiation Pressure Modeling

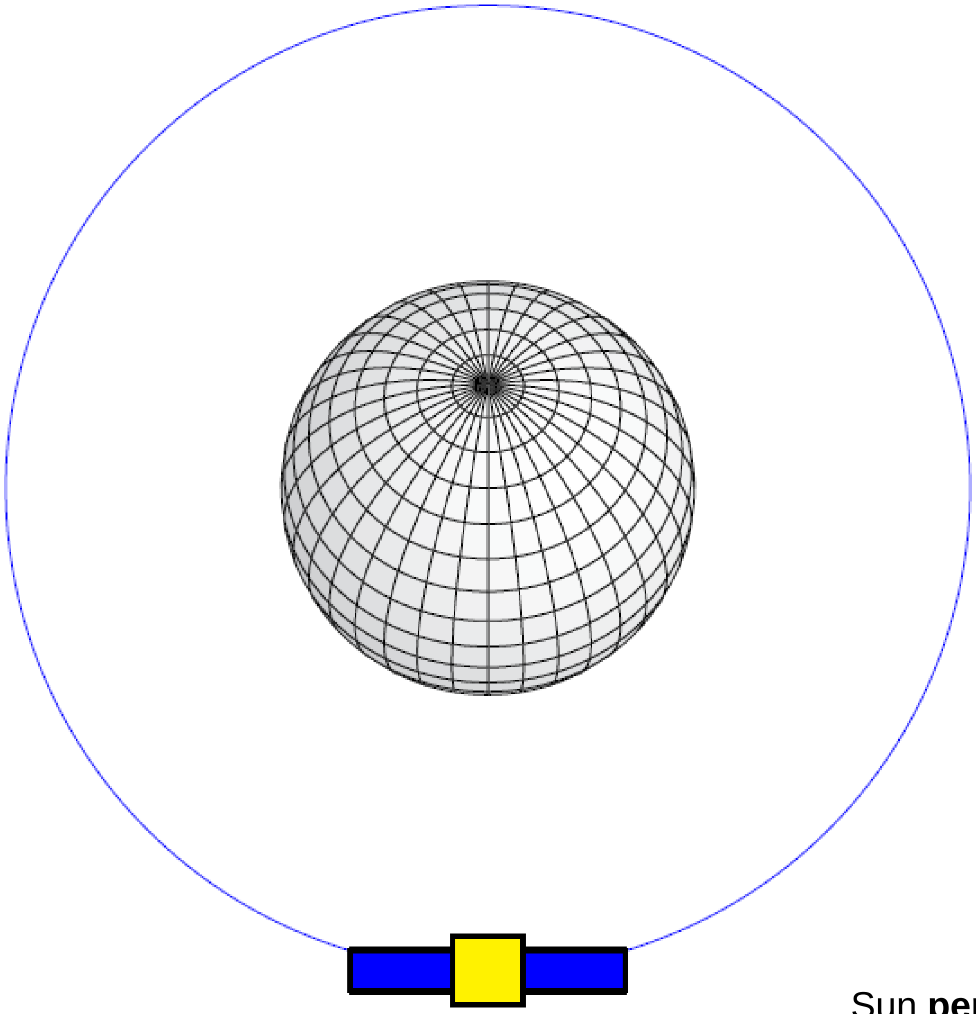

Satellite seen from the Sun,
Sun **perpendicular** to orbital plane.

GNSS Solar Radiation Pressure Modeling

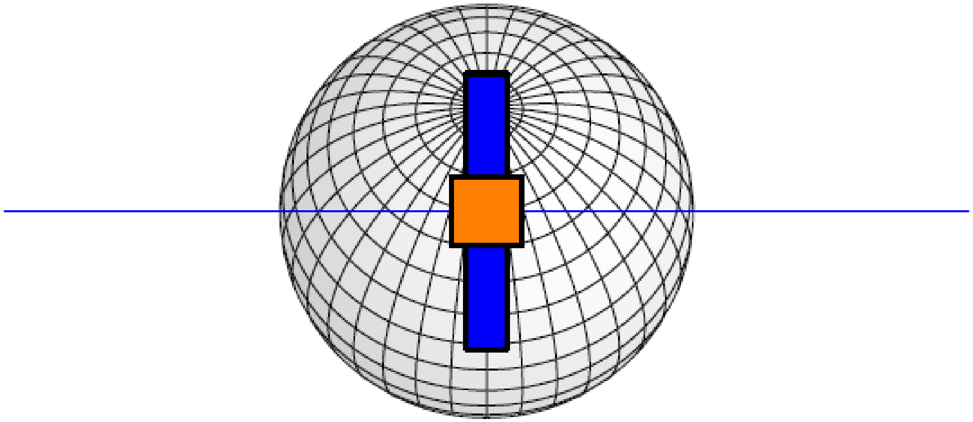

Satellite seen from the Sun,
Sun **lies within** the orbital plane.

GNSS Solar Radiation Pressure Modeling

The following patterns can be recognized:

- The **solar panels** are always pointing to the Sun and thus only cause a constant perturbation in D-direction

- If the Sun is **perpendicular** to the orbital plane, no periodic solar radiation pressure perturbations are expected

- If the Sun is **within** the orbital plane, a twice-per-revolution periodic signal is expected in D-direction (and a once-per-revolution periodic signal in X-direction)

- The more a GNSS satellite body **deviates** from a sphere, the **more pronounced** are the periodic signals (less pronounced for a cube - GPS, more pronounced for a cylinder - Glonass)

New Empirical GNSS Radiation Pressure Model

New Extended CODE Orbit Model (ECOM2) is still represented by

$$\mathbf{a} = \mathbf{a}_0 + D(u)\mathbf{e}_D + Y(u)\mathbf{e}_Y + B(u)\mathbf{e}_B$$

with $\quad \mathbf{e}_D \doteq \dfrac{\mathbf{r}_s - \mathbf{r}}{|\mathbf{r}_s - \mathbf{r}|}, \; \mathbf{e}_Y \doteq -\dfrac{\mathbf{e}_r \times \mathbf{e}_D}{|\mathbf{e}_r \times \mathbf{e}}, \; \mathbf{e}_B \doteq \mathbf{e}_D \times \mathbf{e}_Y \,,$

but now with

$$D(u) = D_0 + \sum_{i=1}^{n_D} \{D_{2i,c} \cos 2i\Delta u + D_{2i,s} \sin 2i\Delta u\}$$

$$Y(u) = Y_0$$

$$B(u) = B_0 + \sum_{i=1}^{n_B} \{B_{2i-1,c} \cos(2i-1)\Delta u + B_{2i-1,s} \sin(2i-1)\Delta u\}$$

$\Delta u = u - u_s$

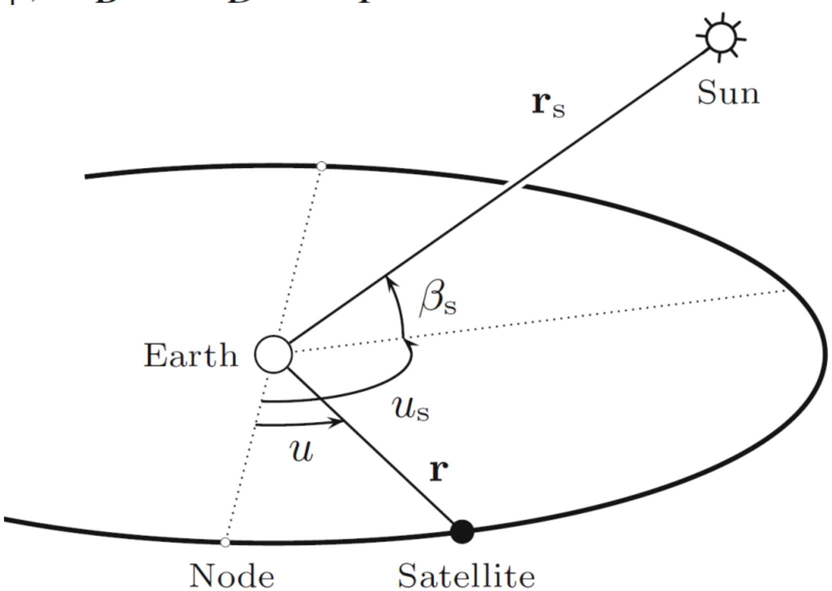

(Arnold et al., 2015)

New GNSS Reprocessing in the frame of EGSIEM

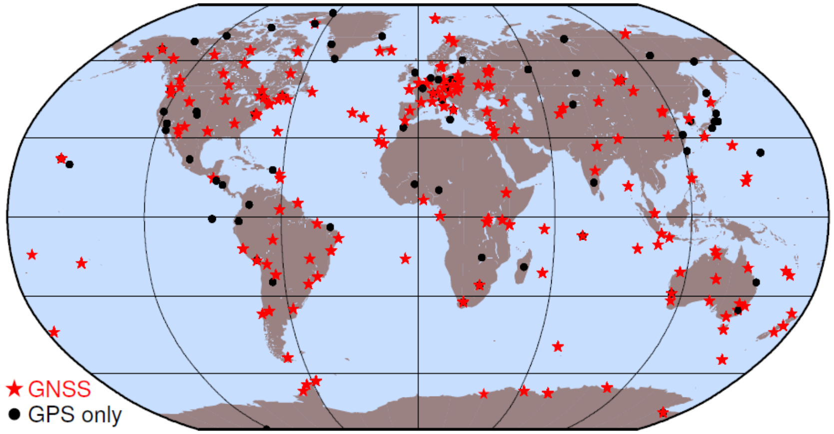

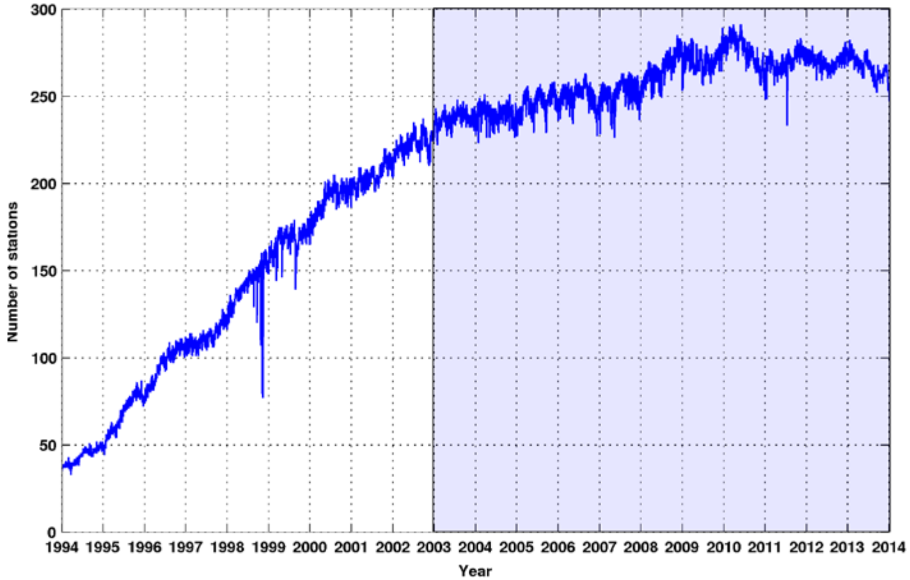

(Sušnik et al., 2017)

- More than 250 globally distributed tracking stations homogeneously reprocessed for 2003-14
- Rigorous combined processing scheme of GPS and GLONASS measurements applied
- Products are GNSS (GPS & GLONASS) **satellite clock corrections** (30-sec, 05-sec), GNSS **satellite orbits**, **Earth rotation parameters**, **station coordinates**

Such products are a prerequisite for LEO POD and gravity field recovery!

GNSS Orbit Validation by Satellite Laser Ranging (SLR)

ECOM2 reduces systematic GNSS orbit errors (GLONASS-M, 2003-14):

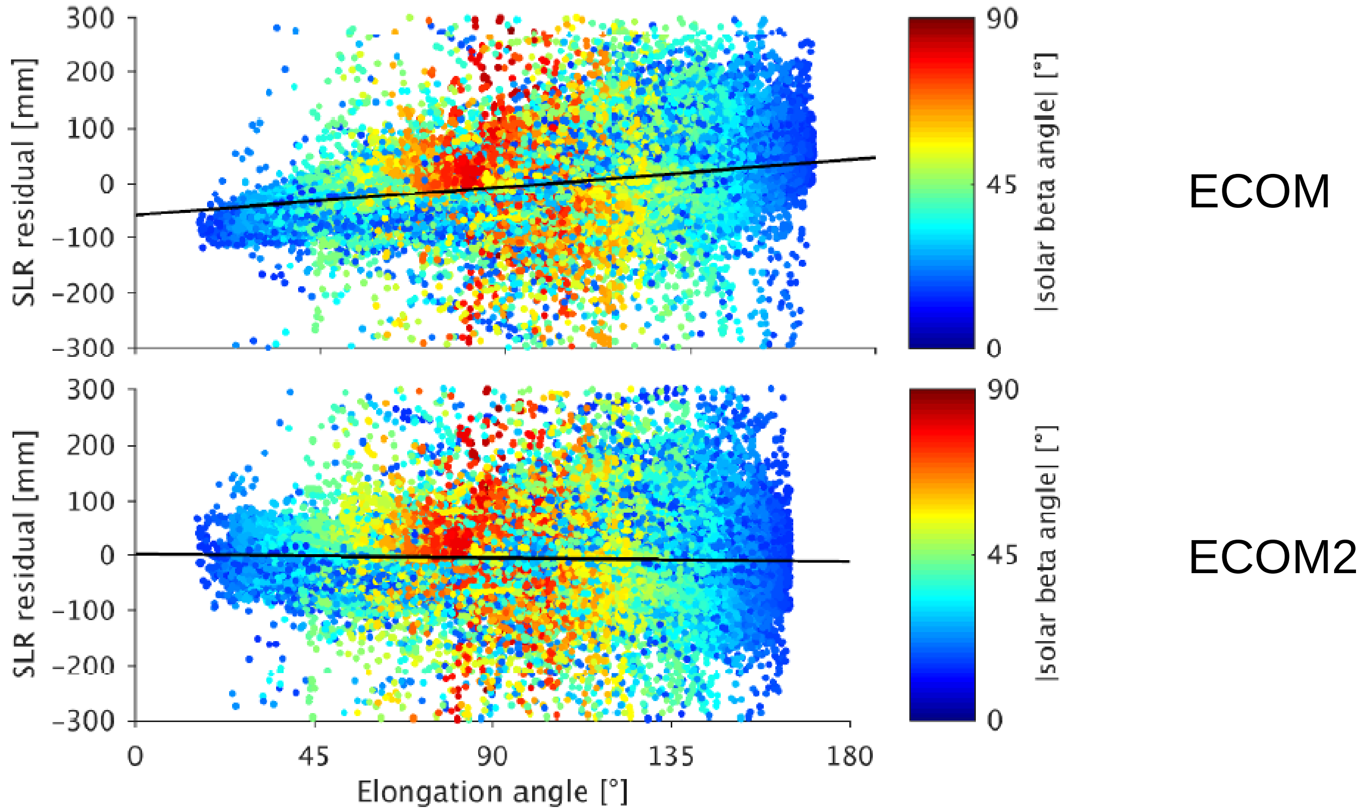

$\cos \varepsilon = \cos \beta \cos \Delta u$

(Sušnik et al., 2017)

Computation of GNSS Clock Corrections

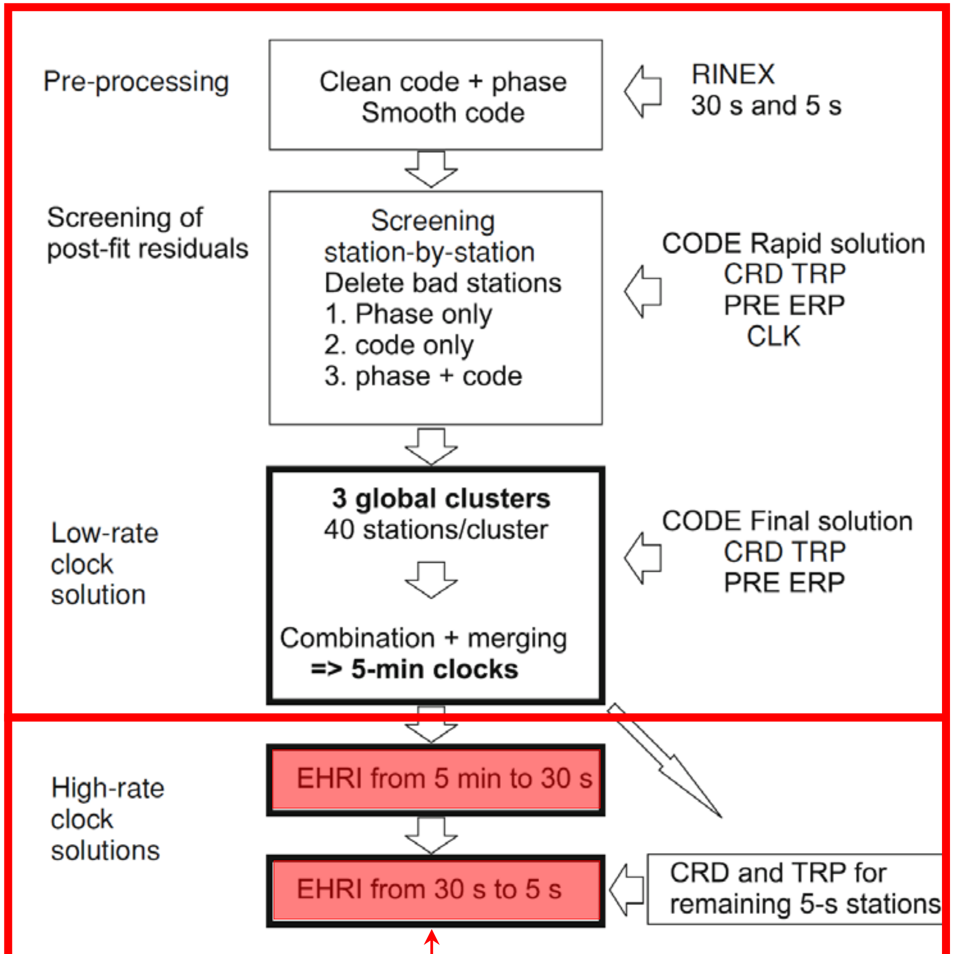

(Bock et al., 2009)

The final clock product with 5 min sampling is based on undifferenced GPS data of typically 120 stations of the IGS network

The IGS 1 Hz network is finally used for clock densification to 5 sec

The 5 sec clocks are interpolated to 1 sec as needed for 1 Hz LEO GPS data

Availability of Reprocessing Products

- All Reprocessing Products covering GPS-only (1994-2001) and combined GPS+GLONASS (2002-2014) are publicly available at

  http://www.aiub.unibe.ch/download/REPRO_2015

- A detailed analysis strategy summary may be found at

  CODE_REPRO_2015.ACN

- The use of the Reprocessing Products should be referenced as

  Sušnik, A., R. Dach, A. Villiger, A. Maier, D. Arnold, S. Schaer, A. Jäggi (2016): CODE reprocessing product series. Published by Astronomical Institute, University of Bern. URL: http://www.aiub.unibe.ch/download/REPRO_2015; DOI: 10.7892/boris.80011

GPS Signals

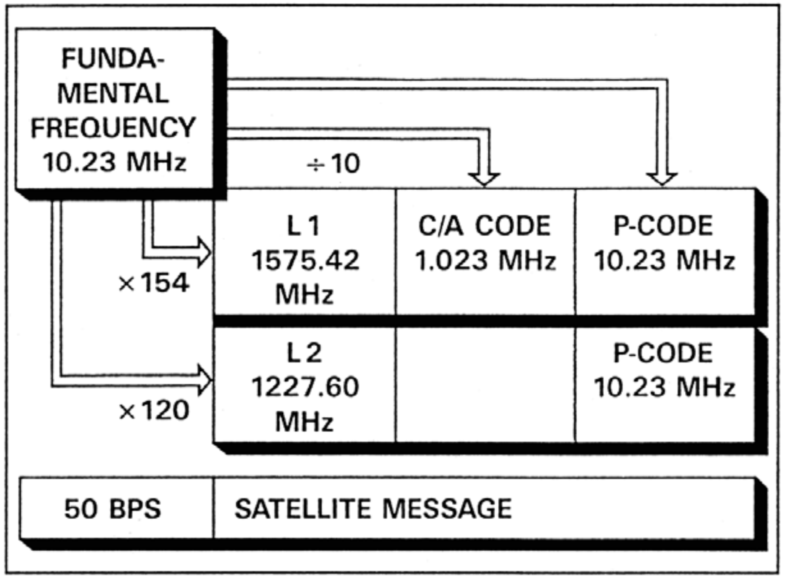

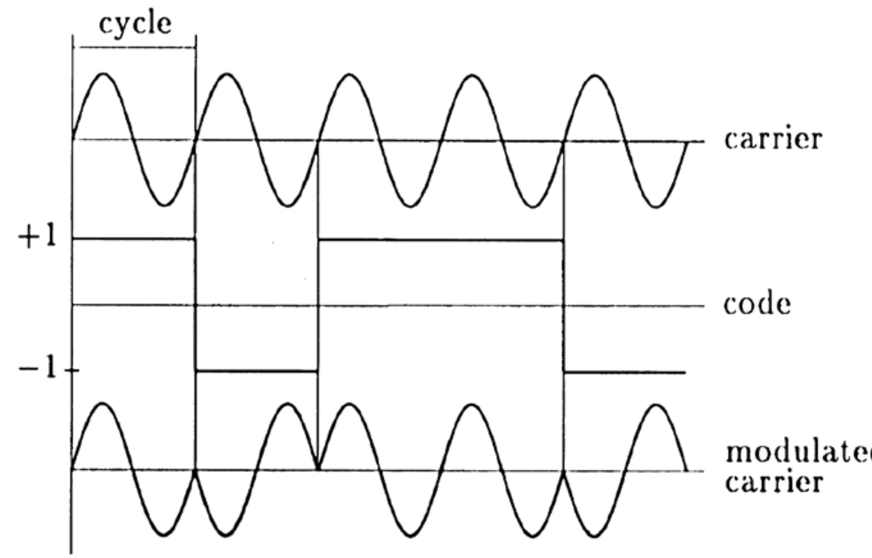

Signals driven by an **atomic clock**

Two **carrier signals** (sine waves):

- **L_1**: f = 1575.43 MHz, λ = 19 cm
- **L_2**: f = 1227.60 MHz, λ = 24 cm

Bits encoded on carrier by phase modulation:

- **C/A-code** (Clear Access / Coarse Acquisition)
- **P-code** (Protected / Precise)
- **Broadcast/Navigation Message**

(e.g. Blewitt, 1997; Teunissen and Montenbruck, 2017)

Carrier Phase Observation Equation

$$L_i^k = \rho_i^k - c \cdot \Delta t^k + c \cdot \Delta t_i + \cancel{T_i^k} + \cancel{I_i^k} + \lambda \cdot N_i^k$$
$$+ \Delta_{rel} - c \cdot b^k + c \cdot b_i + m_i^k + \epsilon_i^k$$

ρ_i^k	Distance between satellite and receiver	Satellite positions and clocks
Δt^k	Satellite clock offset wrt GPS time	are known from ACs or IGS
Δt_i	Receiver clock offset wrt GPS time	
$\cancel{T_i^k}$	~~Tropospheric delay~~	Not existent for LEOs
$\cancel{I_i^k}$	~~Ionospheric delay~~	Cancels out (first order only) when forming the ionosphere-free linear combination:
N_i^k	Phase ambiguity	
Δ_{rel}	Relativistic corrections	
b^k	Delays in satellite (cables, electronics)	
b_i	Delays in receiver and antenna	
m_i^k	Multipath, scattering, bending effects	
ϵ_i^k	Measurement error	

$$L_c = \frac{f_1^2}{f_1^2 - f_2^2} L_1 - \frac{f_2^2}{f_1^2 - f_2^2} L_2$$

Geometric Distance

Geometric distance ρ_{leo}^{k} is given by:

$$\rho_{leo}^{k} = \left|\boldsymbol{r}_{leo}(t_{leo}) - \boldsymbol{r}^{k}(t_{leo} - \tau_{leo}^{k})\right|$$

$\boldsymbol{r}_{leo}$ Inertial position of LEO antenna phase center at reception time

$\boldsymbol{r}^{k}$ Inertial position of GPS antenna phase center of satellite k at emission time

τ_{leo}^{k} Signal traveling time between the two phase center positions

Different ways to represent $\boldsymbol{r}_{leo}$:

- **Kinematic** orbit representation
- **Dynamic** or **reduced-dynamic** orbit representation

Kinematic Orbit Representation

Satellite position $\boldsymbol{r}_{leo}(t_{leo})$ (in inertial frame) is given by:

$$\boldsymbol{r}_{leo}(t_{leo}) = \boldsymbol{R}(t_{leo}) \cdot (\boldsymbol{r}_{leo,e,0}(t_{leo}) + \delta\boldsymbol{r}_{leo,e,ant}(t_{leo}))$$

$\boldsymbol{R}$	Transformation matrix from Earth-fixed to inertial frame
$\boldsymbol{r}_{leo,e,0}$	LEO center of mass position in Earth-fixed frame
$\delta\boldsymbol{r}_{leo,e,ant}$	LEO antenna phase center offset in Earth-fixed frame

Kinematic positions $\boldsymbol{r}_{leo,e,0}$ are estimated for each **measurement epoch**:

- Measurement epochs **need not** to be identical with nominal epochs
- Positions are **independent** of models describing the LEO dynamics. Velocities cannot be provided

Kinematic Orbit Representation

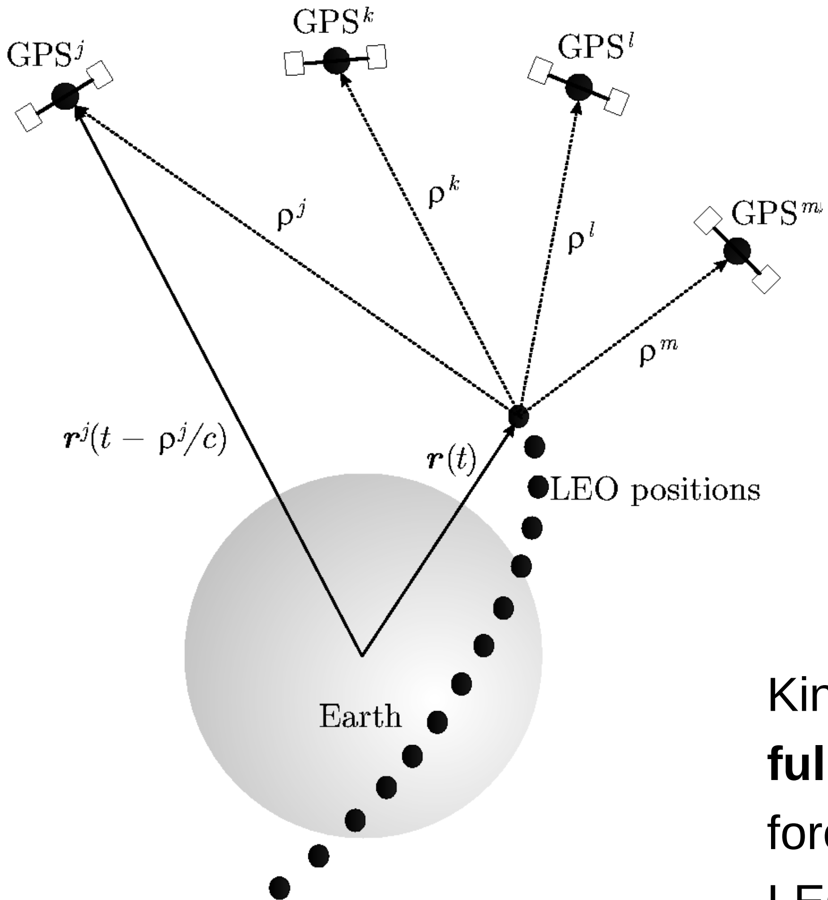

A kinematic orbit is an ephemeris at **discrete** measurement epochs

Kinematic positions are **fully independent** on the force models used for LEO orbit determination

(Švehla and Rothacher, 2004)

Kinematic Orbit Representation

Measurement epochs
(in GPS time)

Positions (km)
(Earth-fixed)

*	2016	6	1	0	0	17.99999974
PL49	-2023.517746	-3061.130332	5742.844473	0.262691		
*	2016	6	1	0	0	18.99999989
PL49	-2026.734429	-3066.703833	5738.746569	0.111976		
*	2016	6	1	0	0	19.99999974
PL49	-2029.949393	-3072.273033	5734.641440	0.261262		
*	2016	6	1	0	0	20.99999979
PL49	-2033.162630	-3077.837924	5730.529099	0.210548		
*	2016	6	1	0	0	21.99999984
PL49	-2036.374136	-3083.398504	5726.409546	0.159835		
*	2016	6	1	0	0	22.99999979
PL49	-2039.583909	-3088.954755	5722.282787	0.209119		
*	2016	6	1	0	0	23.99999984
PL49	-2042.791949	-3094.506686	5718.148843	0.158440		
*	2016	6	1	0	0	24.99999979
PL49	-2045.998248	-3100.054291	5714.007709	0.207778		
*	2016	6	1	0	0	25.99999974
PL49	-2049.202791	-3105.597545	5709.859370	0.257064		
*	2016	6	1	0	0	26.99999979
PL49	-2052.405584	-3111.136450	5705.703844	0.206352		

Clock correction to nominal epoch (μs), e.g., to epoch 00:00:20

Excerpt of kinematic Swarm-C positions at begin of 1 June, 2016

Dynamic Orbit Representation

Satellite position $\boldsymbol{r}_{leo}(t_{leo})$ (in inertial frame) is given by:

$$\boldsymbol{r}_{leo}(t_{leo}) = \boldsymbol{r}_{leo,0}(t_{leo}; a, e, i, \Omega, \omega, u_0; Q_1, ..., Q_d) + \delta\boldsymbol{r}_{leo,ant}(t_{leo})$$

$\boldsymbol{r}_{leo,0}$	LEO center of mass position
$\delta\boldsymbol{r}_{leo,ant}$	LEO antenna phase center offset
$a, e, i, \Omega, \omega, u_0$	LEO initial osculating orbital elements
$Q_1, ..., Q_d$	LEO dynamical parameters

Satellite trajectory $\boldsymbol{r}_{leo,0}$ is a particular solution of an **equation of motion**

- One set of **initial conditions** (orbital elements) is estimated per arc.
  Dynamical parameters of the force model are estimated on request.

Dynamic Orbit Representation

Equation of motion (in inertial frame) is given by:

$$\ddot{\boldsymbol{r}} = -GM\frac{\boldsymbol{r}}{r^3} + \boldsymbol{f}_1(t, \boldsymbol{r}, \dot{\boldsymbol{r}}, Q_1, ..., Q_d)$$

with initial conditions

$$\boldsymbol{r}(t_0) = \boldsymbol{r}(a, e, i, \Omega, \omega, u_0; t_0)$$
$$\dot{\boldsymbol{r}}(t_0) = \dot{\boldsymbol{r}}(a, e, i, \Omega, \omega, u_0; t_0)$$

The **acceleration** $\boldsymbol{f}_1$ consists of **gravitational** and **non-gravitational** perturbations taken into account to model the satellite trajectory. Unknown parameters $Q_1, ..., Q_d$ of force models may appear in the equation of motion together with deterministic (known) accelerations given by analytical models.

Osculating Orbital Elements

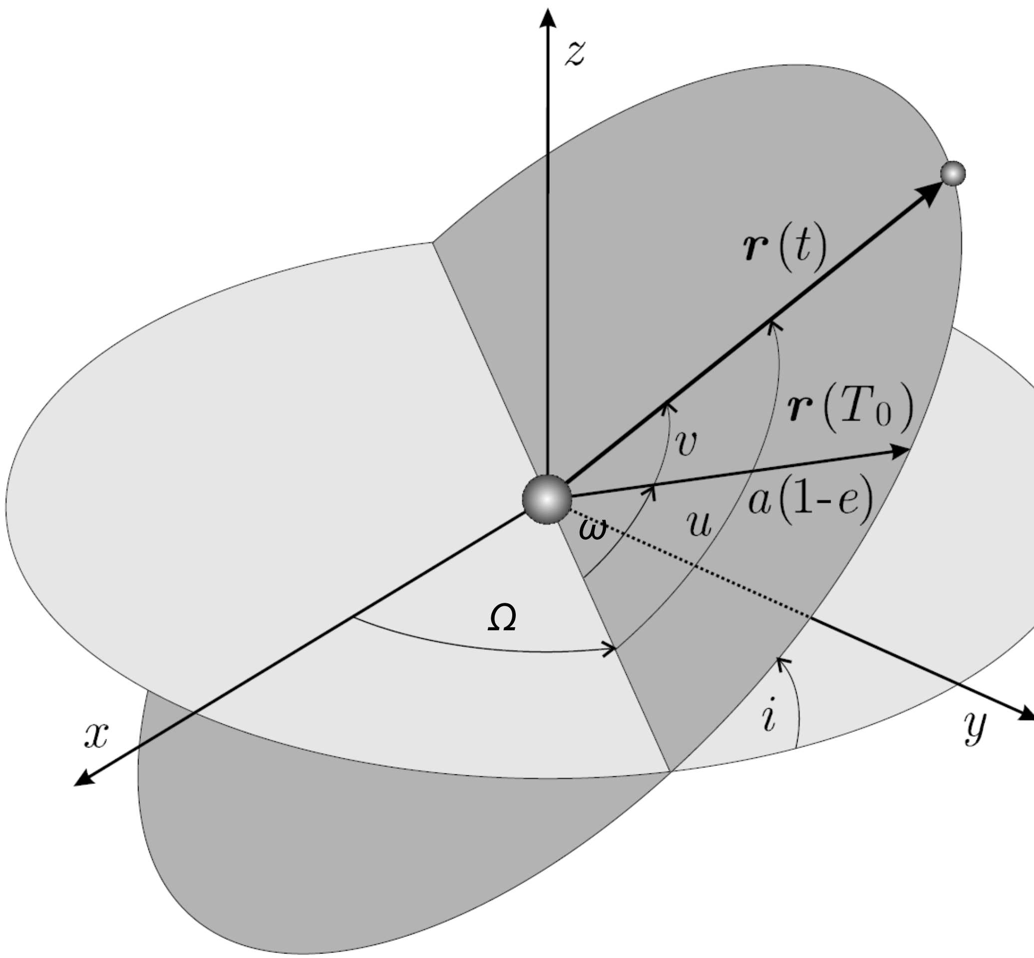

(Beutler, 2005)

Perturbing Accelerations of a LEO Satellite

Force	**Acceleration** (m/s²)
Central term of Earth's gravity field	8.42
Oblateness of Earth's gravity field	0.015
Atmospheric drag	0.00000079
Higher order terms of Earth's gravity field	0.00025
Attraction from the Moon	0.0000054
Attraction from the Sun	0.0000005
Direct solar radiation pressure	0.000000097
...	...

Accurate non-gravitational force modeling is challenging and currently exploited for the various satellites of the Sentinel constellation. For gravity missions the non-gravitational accelerations are measured with on-board accelerometers.

Dynamic Orbit Representation

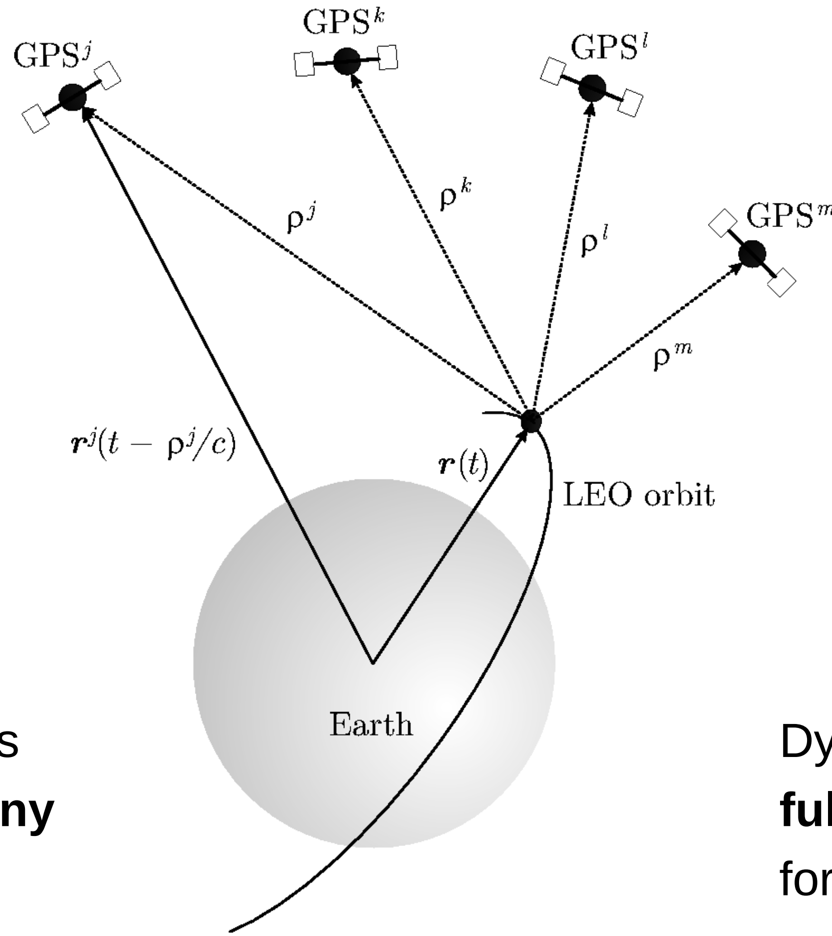

Dynamic orbit positions may be computed at **any epoch** within the arc

Dynamic positions are **fully dependent** on the force models used, e.g., on the gravity field model

Reduced-Dynamic Orbit Representation

Equation of motion (in inertial frame) is given by:

$$\ddot{\boldsymbol{r}} = -GM\frac{\boldsymbol{r}}{r^3} + \boldsymbol{f}_1(t, \boldsymbol{r}, \dot{\boldsymbol{r}}, Q_1, ..., Q_d, P_1, ..., P_s)$$

$P_1, ..., P_s$ Pseudo-stochastic parameters

Pseudo-stochastic parameters are:

- additional empirical parameters characterized by a priori known **statistical properties**, e.g., by expectation values and a priori variances

- useful to **compensate** for deficiencies in dynamic models, e.g., deficiencies in models describing non-gravitational accelerations

- often set up as **piecewise constant accelerations** to ensure that satellite trajectories are continuous and differentiable at any epoch

Reduced-Dynamic Orbit Representation

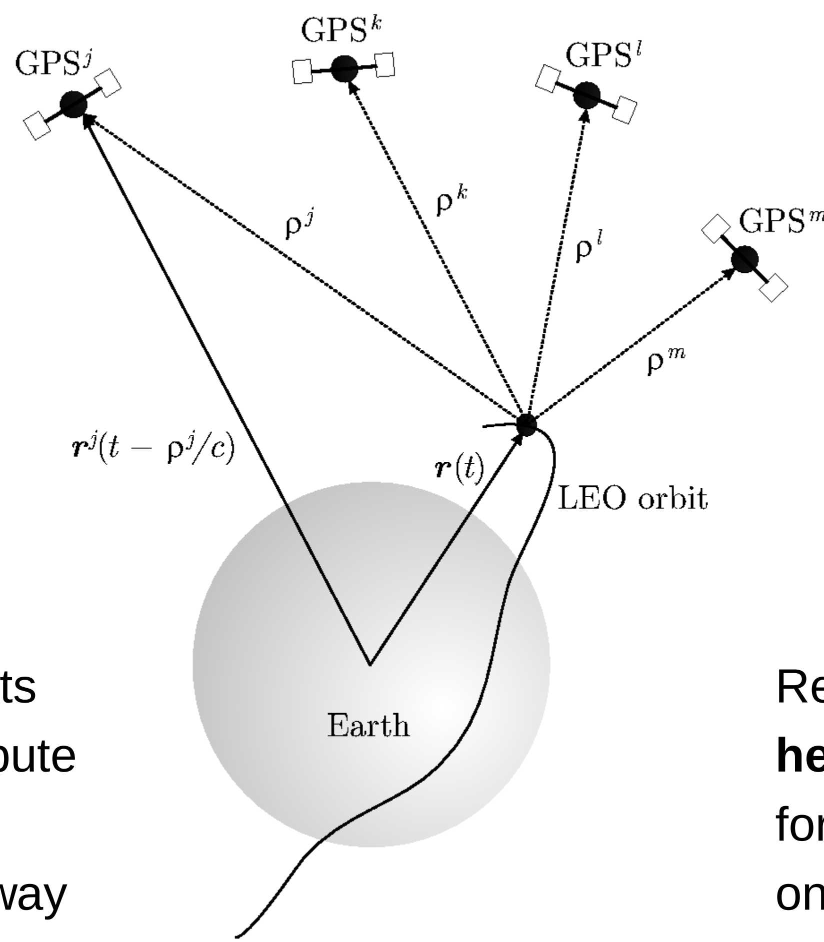

Reduced-dynamic orbits are well suited to compute LEO orbits of **highest quality** in an efficient way (e.g. Jäggi et al., 2017)

Reduced-dynamic orbits **heavily depend** on the force models used, e.g., on the gravity field model

(Jäggi et al., 2008)

Reduced-dynamic Orbit Representation

Position epochs
(in GPS time)

Positions (km) &
Velocities (dm/s)
(Earth-fixed)

Clock corrections
are not provided

```
*  2016  6  1  0  0  0.00000000
PL49  -1965.328762  -2960.079621   5815.366063 999999.999999
VL49 -32476.530949 -56518.428574 -39633.949261 999999.999999
*  2016  6  1  0  0 10.00000000
PL49  -1997.722965  -3016.388318   5775.367094 999999.999999
VL49 -32311.097194 -56097.834133 -40363.154274 999999.999999
*  2016  6  1  0  0 20.00000000
PL49  -2029.949403  -3072.273033   5734.641439 999999.999999
VL49 -32141.000143 -55670.464832 -41087.301898 999999.999999
*  2016  6  1  0  0 30.00000000
PL49  -2062.003415  -3127.727011   5693.194205 999999.999999
VL49 -31966.250891 -55236.380456 -41806.300697 999999.999999
*  2016  6  1  0  0 40.00000000
PL49  -2093.880357  -3182.743574   5651.030585 999999.999999
VL49 -31786.861194 -54795.641569 -42520.059993 999999.999999
*  2016  6  1  0  0 50.00000000
PL49  -2125.575594  -3237.316095   5608.155863 999999.999999
VL49 -31602.843520 -54348.309592 -43228.489711 999999.999999
*  2016  6  1  0  1  0.00000000
PL49  -2157.084506  -3291.438018   5564.575411 999999.999999
VL49 -31414.211010 -53894.446726 -43931.500489 999999.999999
```

Excerpt of reduced-dynamic Swarm-C positions at begin of 1 June, 2016

LEO Sensor Offsets

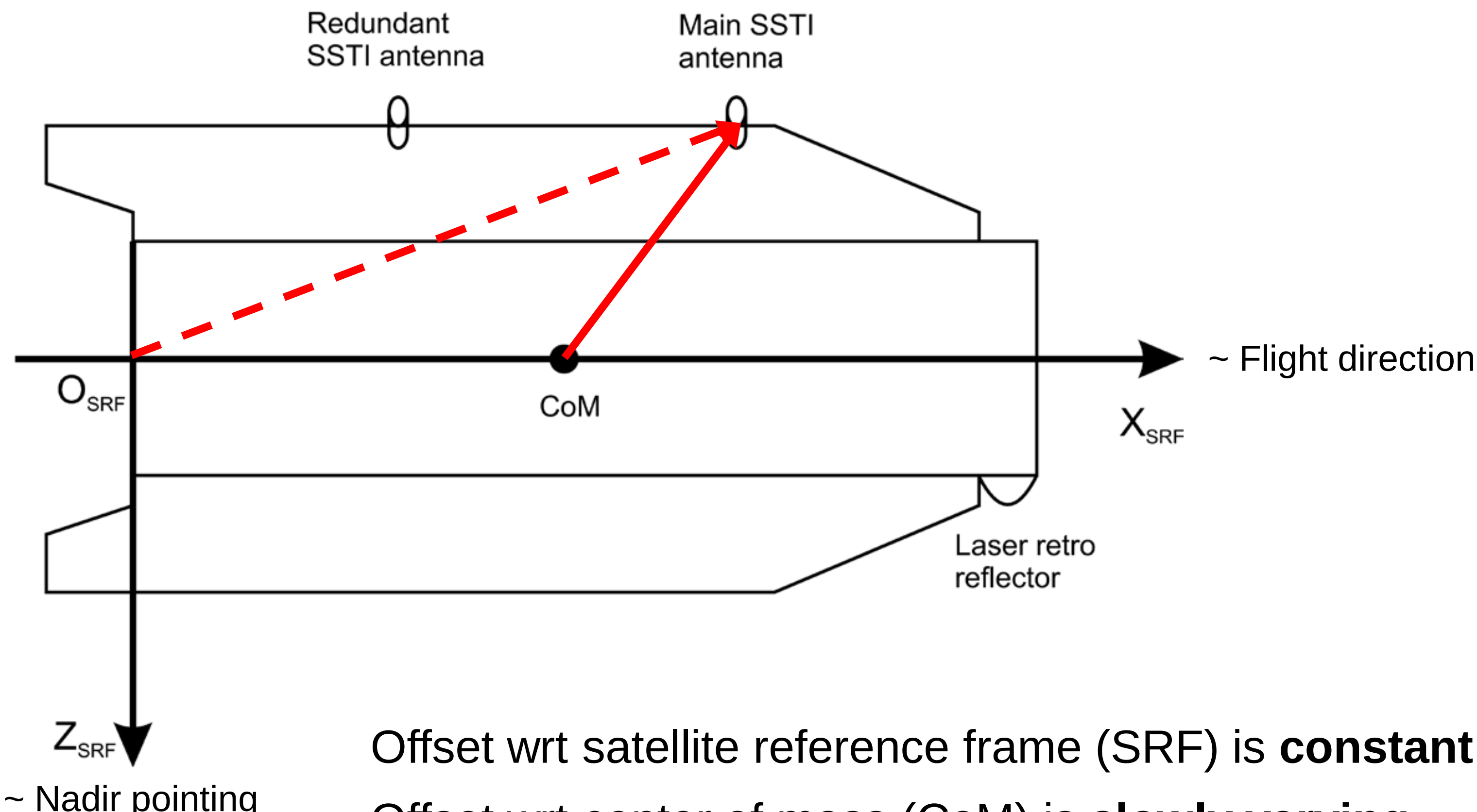

Offset wrt satellite reference frame (SRF) is **constant**

Offset wrt center of mass (CoM) is **slowly varying**

LEO Sensor Offsets

Phase center offsets $\delta \boldsymbol{r}_{leo,ant}$:

- are needed in the inertial or Earth-fixed frame and have to be transformed from the satellite frame using **attitude data** from the star-trackers
- consist of a frequency-independent **instrument offset**, e.g., defined by the center of the instrument‘s mounting plane (CMP) in the satellite frame
- consist of frequency-dependent **phase center offsets** (PCOs), e.g., defined wrt the center of the instrument‘s mounting plane in the antenna frame (ARF)
- consist of frequency-dependent **phase center variations** (PCVs) varying with the direction of the incoming signal, e.g., defined wrt the PCOs in the antenna frame

Spaceborne GPS Antennas: GOCE

L1, L2, Lc phase center offsets

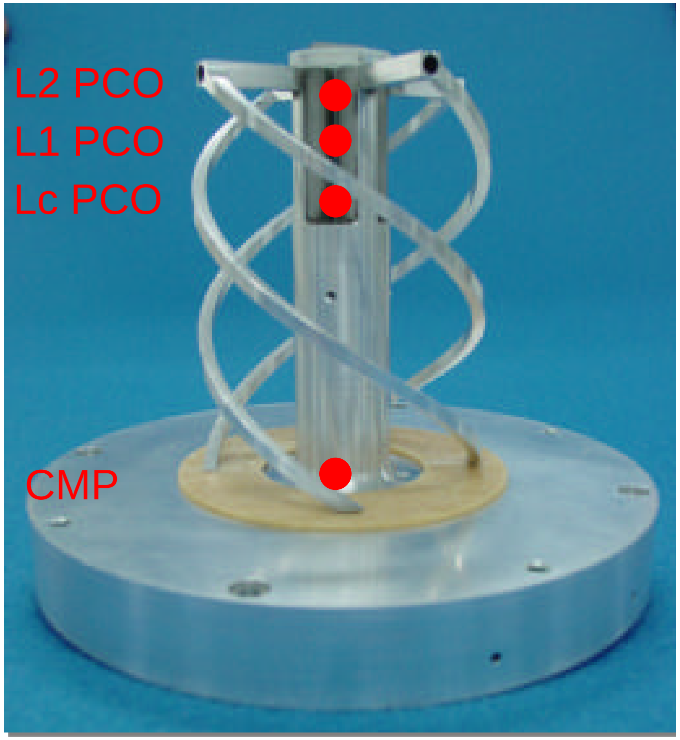

Measured from ground calibration in anechoic chamber

Lc phase center variations

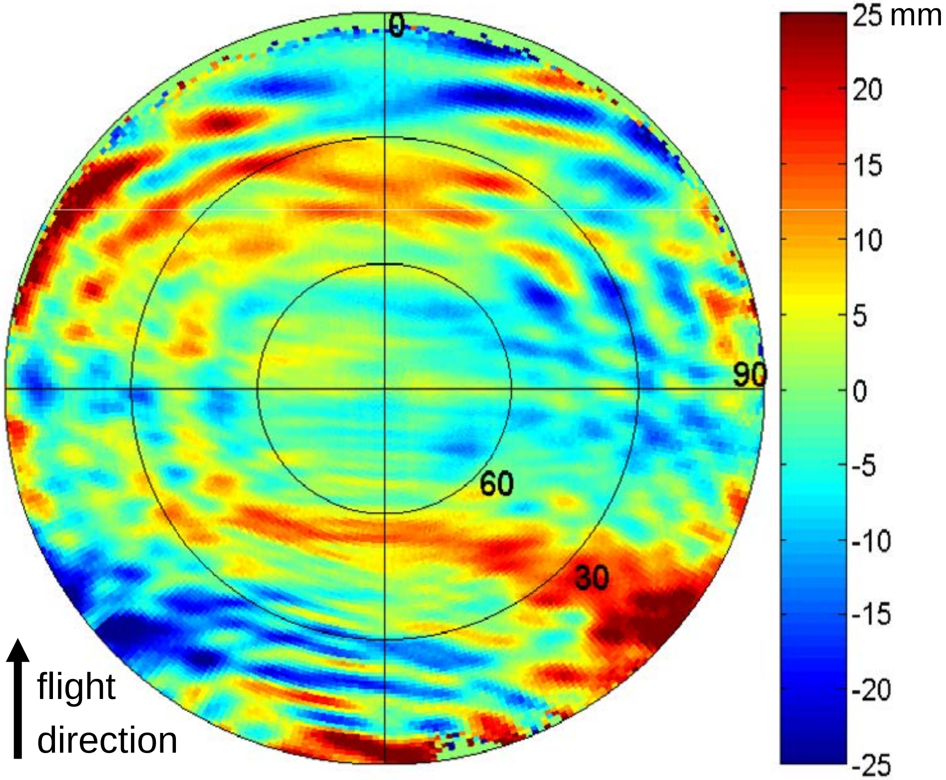

Empirically derived during orbit determination according to Jäggi et al. (2009)

Spaceborne GPS Antennas: Swarm

Swarm GPS antenna

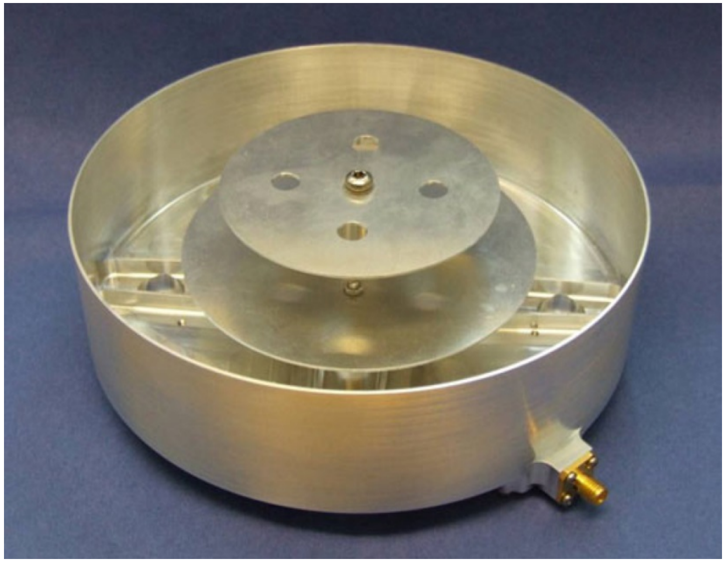

Multipath shall be minimzed by chokering

L_{if} phase center variations

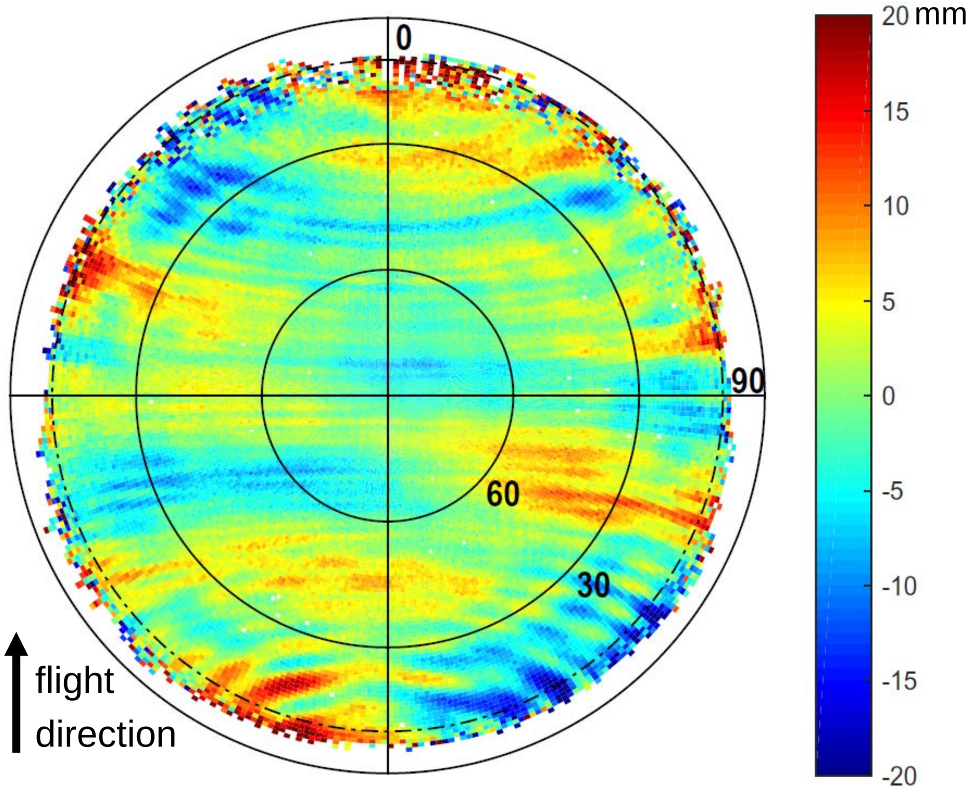

Empirically derived during orbit determination according to Jäggi et al. (2009)

Spaceborne GPS Antennas: GRACE

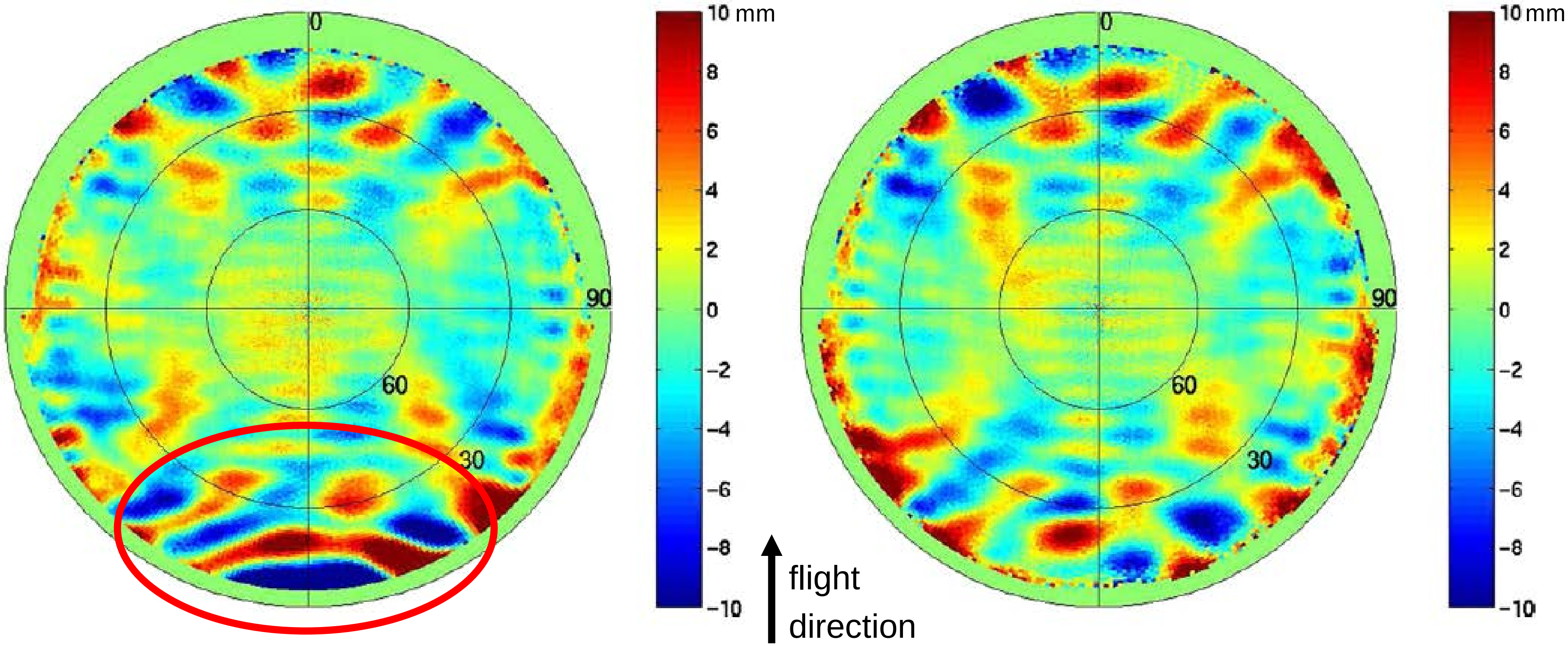

GRACE-A
(occultation antenna switched on)

GRACE-B

(Jäggi et al., 2009)

Visualization of Orbit Solutions

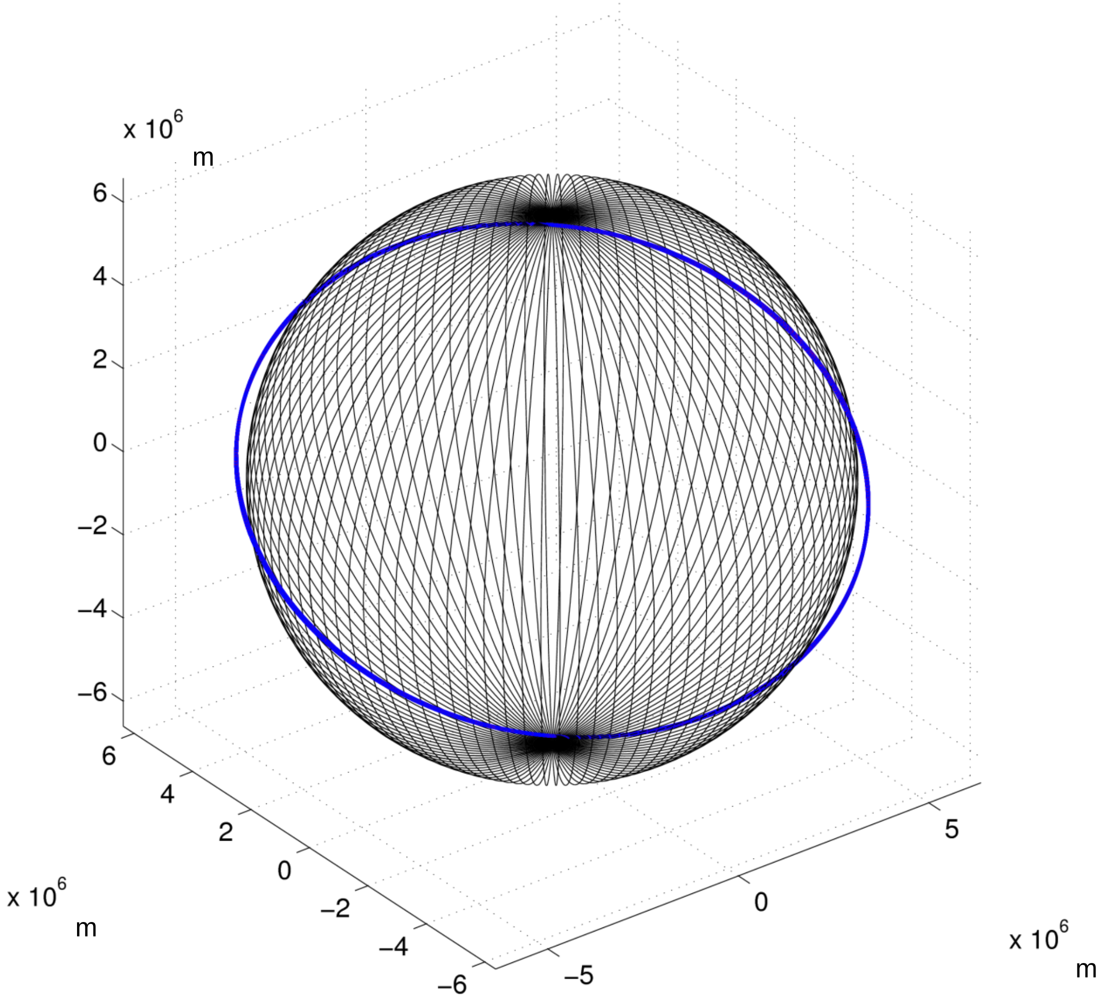

It is more instructive to look at differences between orbits in well suited coordinate systems …

Co-Rotating Orbital Frames

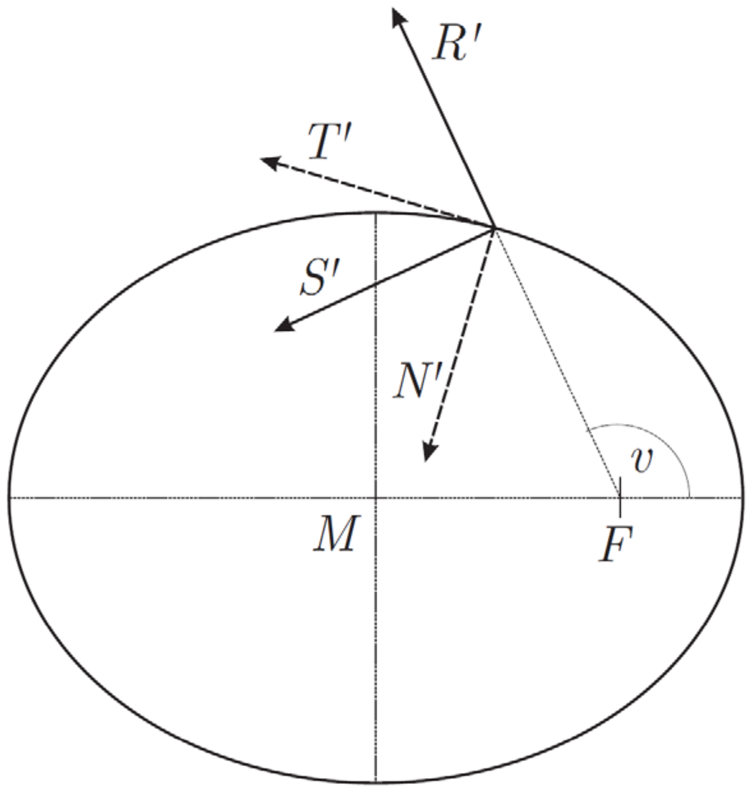

R, S, C unit vectors are pointing:

- into the radial direction
- normal to **R** in the orbital plane
- normal to the orbital plane (cross-track)

T, N, C unit vectors are pointing:

- into the tangential (along-track) direction
- normal to **T** in the orbital plane
- normal to the orbital plane (cross-track)

Small eccentricities: **S**~**T** (velocity direction)

(Beutler, 2005)

Orbit Differences KIN-RD (Swarm-C)

Differences at epochs of kin. positions

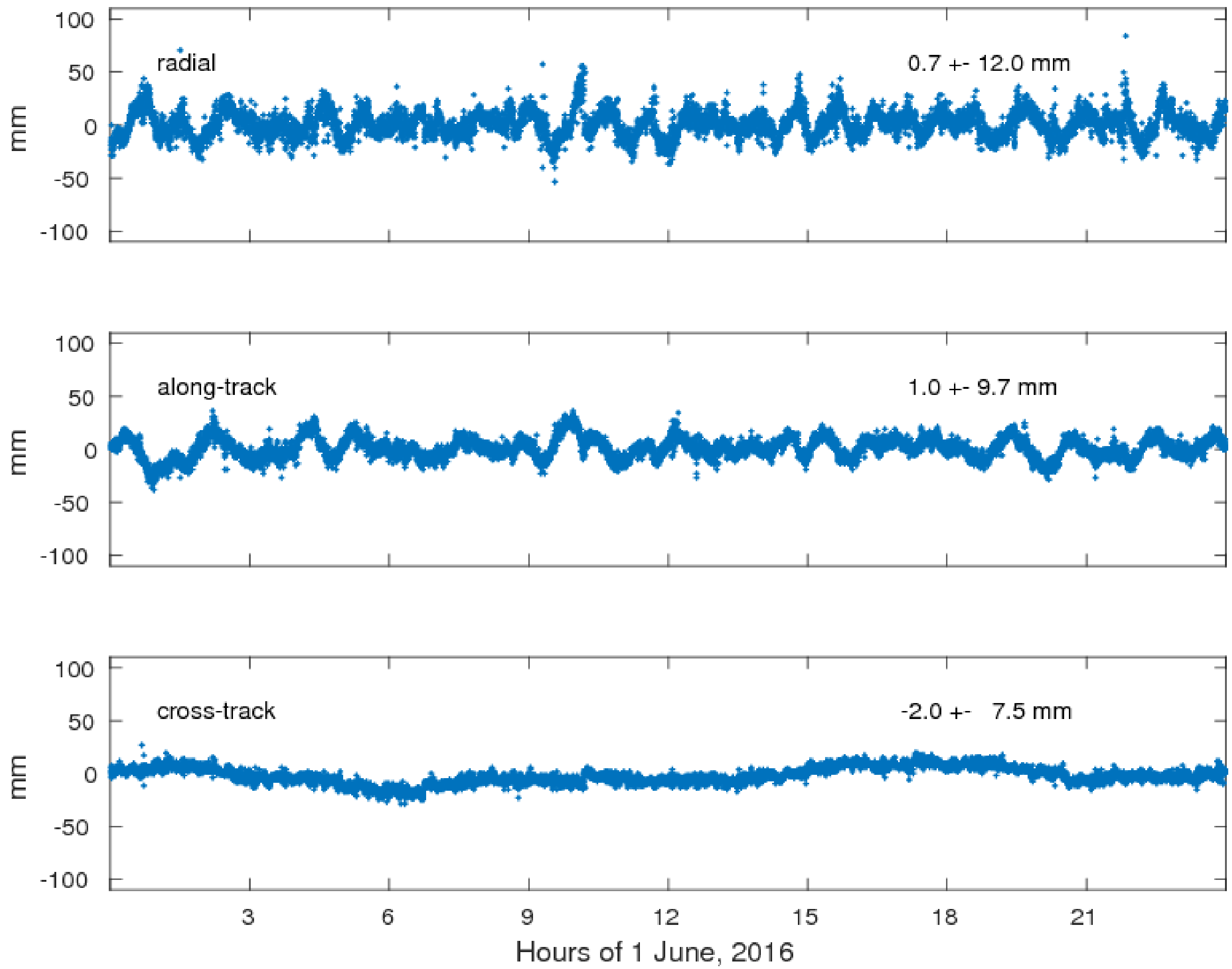

Orbit Comparisons (Sentinel-1A)

Radial

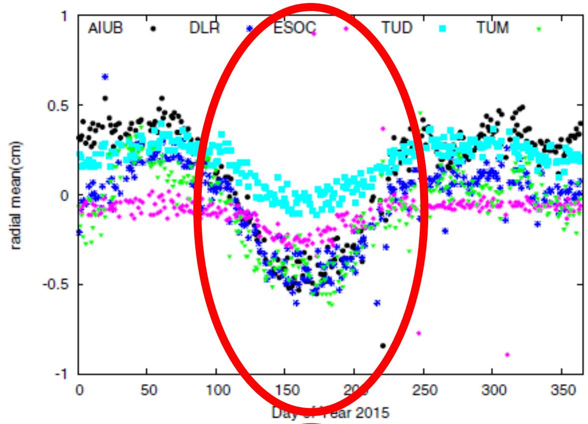

Along-track

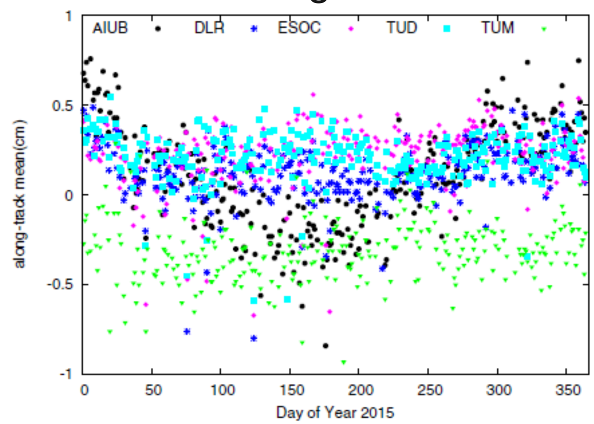

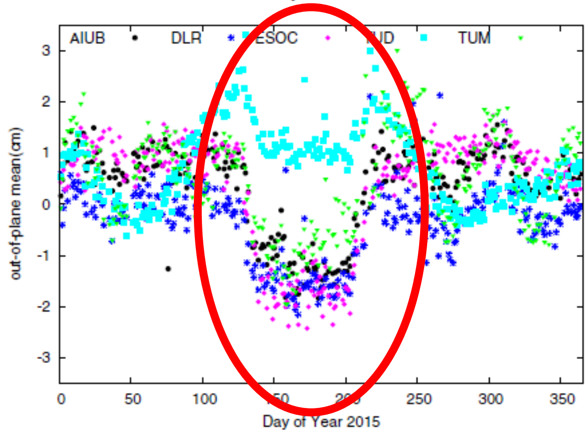

Cross-track

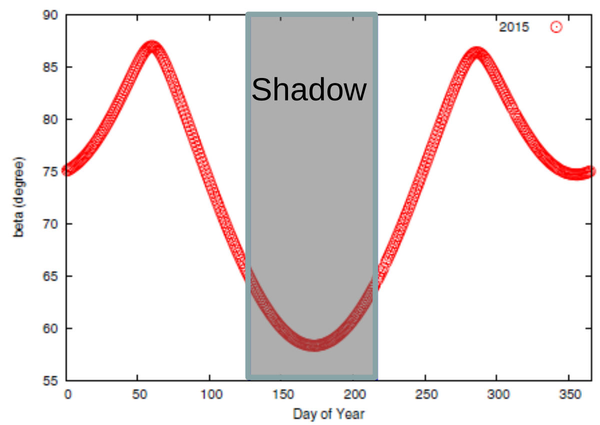

β-angle

- Shown are daily mean differences between various POD centers
- Systematics are revealed due to different modeling approaches
- Comparisons help to understand the strengths and the weaknesses of the more dynamic and the more kinematic POD approaches

(Peter et al., 2017)

Pseudo-Stochastic Accelerations (GOCE)

First drag-free flight on 7 May

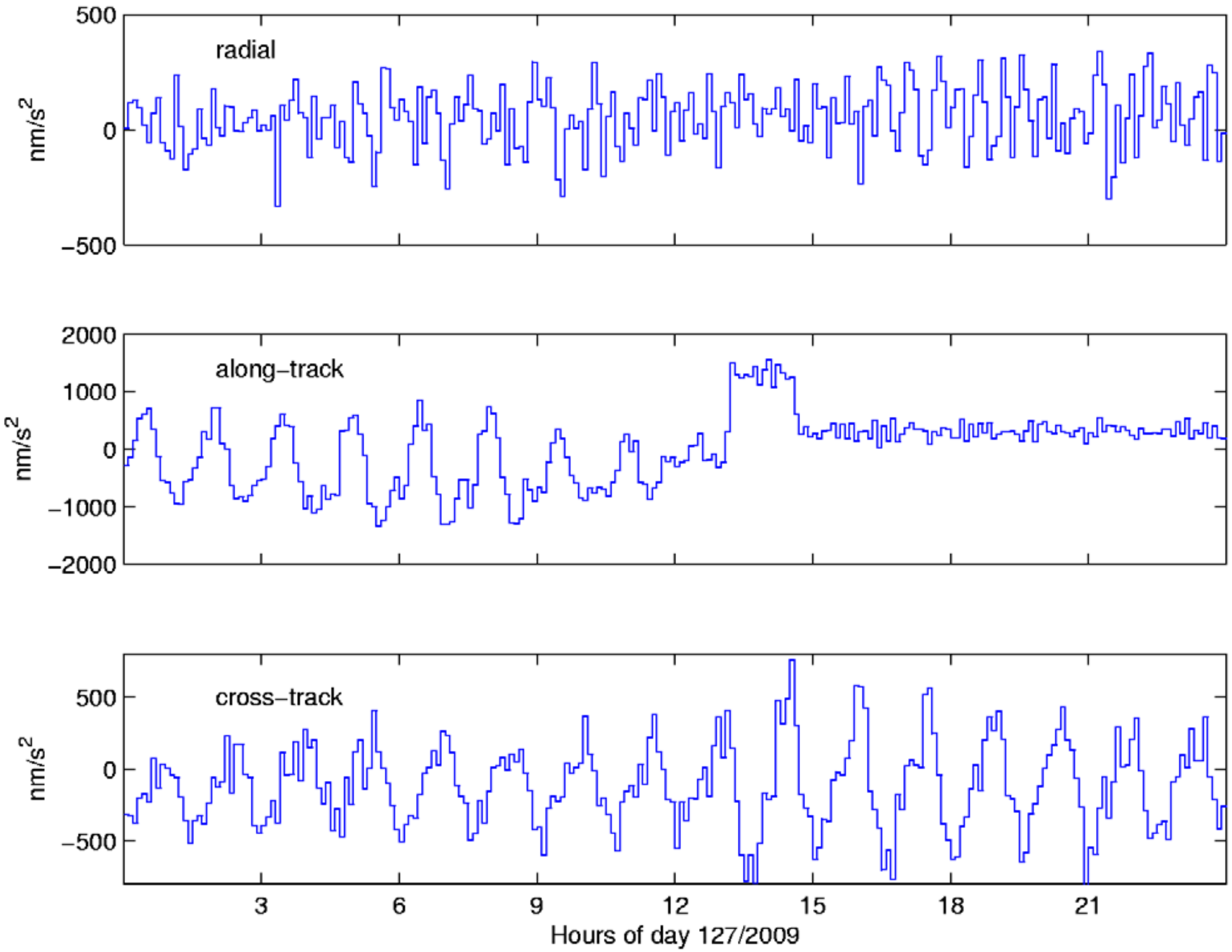

Impact of New Reprocessing Products

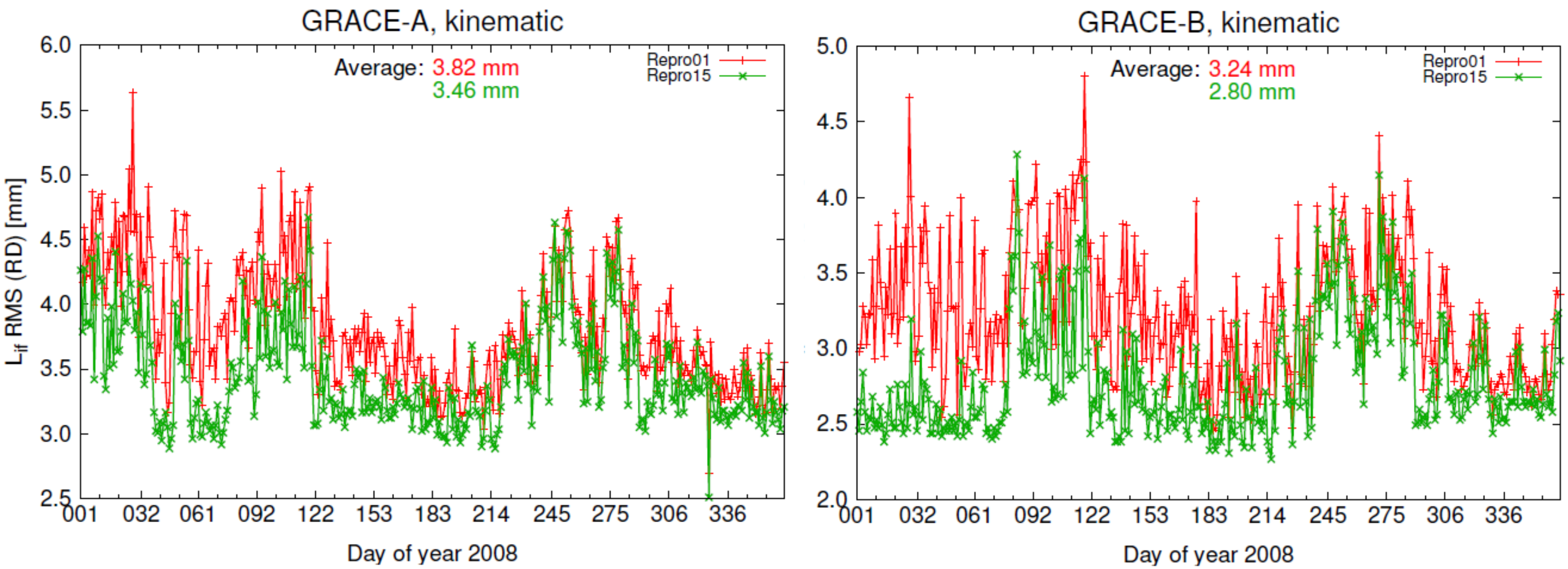

(RMS of fit of ionosphere-free carrier phase measurements)

Reduction of carrier phase residuals of GRACE kinematic positions due to the new reprocessing products.

(Sušnik et al., 2017)

Ionospheric (Side-) Effects in GPS Data

For GOCE systematic effects around the geomagnetic equator were observed in the ionosphere-free GPS phase residuals **=> affects kinematic positions**

Degradation of kinematic positions around the geomagnetic equator propagates into gravity field solutions.

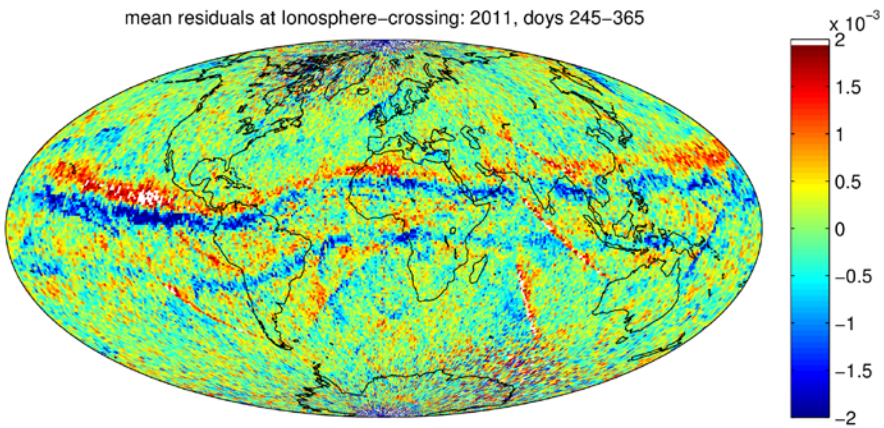

Phase observation residuals (- 2 mm … +2 mm) mapped to the ionosphere piercing point

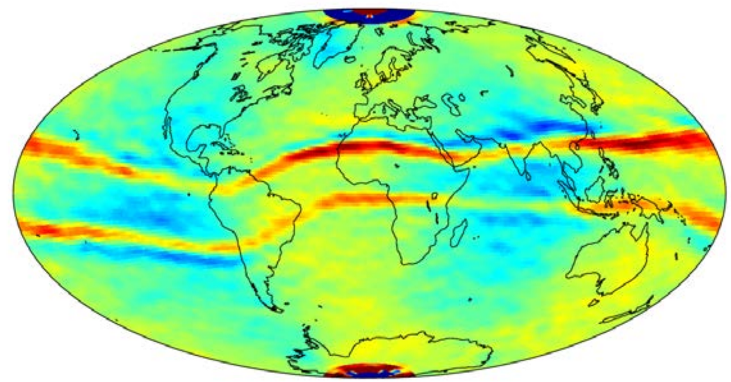

Geoid height differences (−5 cm … 5 cm);
R4 period

(Jäggi et al., 2015)

Situation for Swarm

Original GPS Data
(13 months)

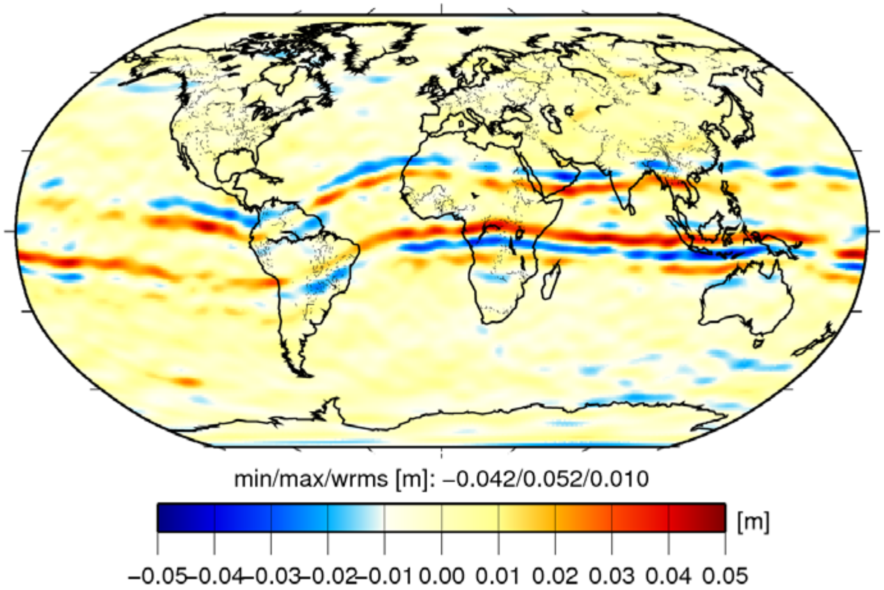

Screened GPS Data
(18 months)

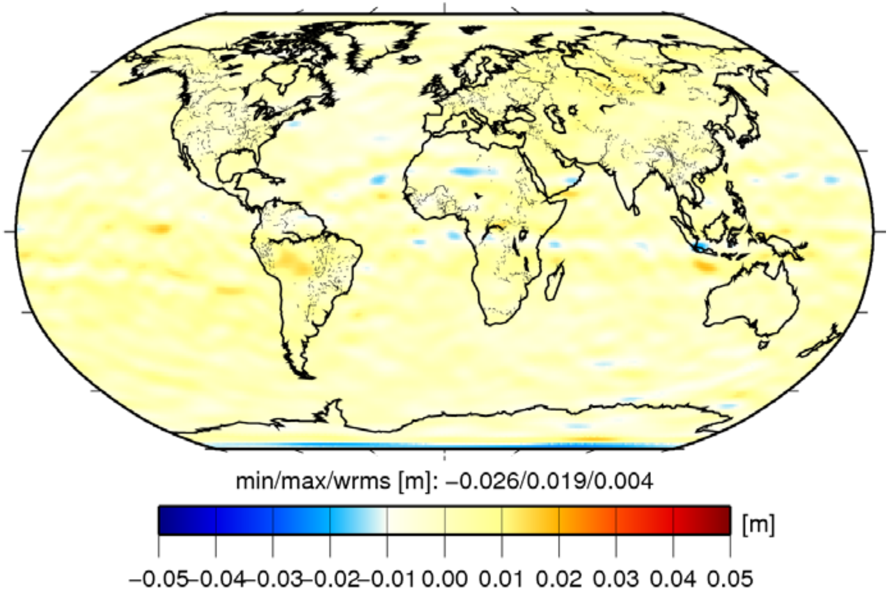

(Differences wrt GOCO05S, 400 km Gauss smoothing adopted)

Systematic signatures along the geomagnetic equator may be efficiently reduced for static Swarm gravity field recovery when screening the raw RINEX GPS data files with a ΔL_{gf} criterion.

(Jäggi et al., 2016)

Situation for GRACE

Original GPS Data
(Swarm)

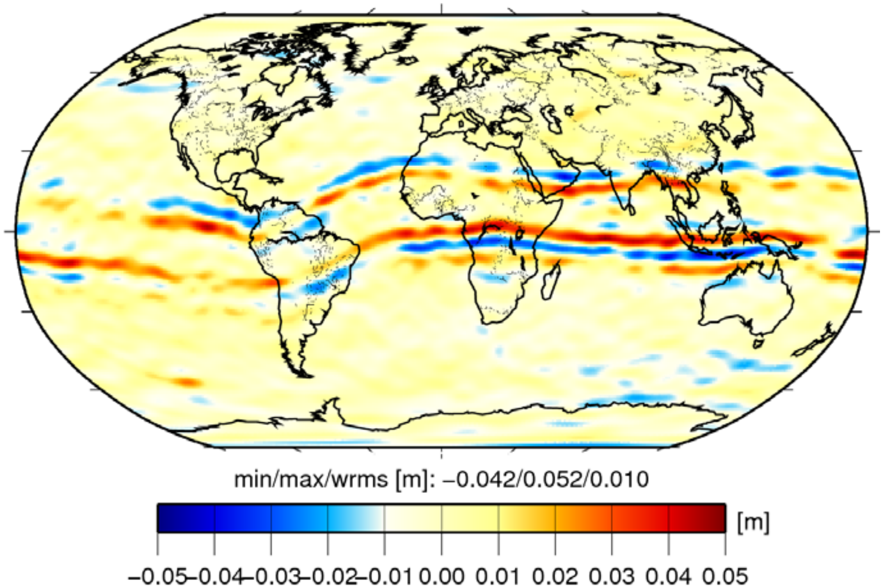

Original GPS Data
(GRACE)

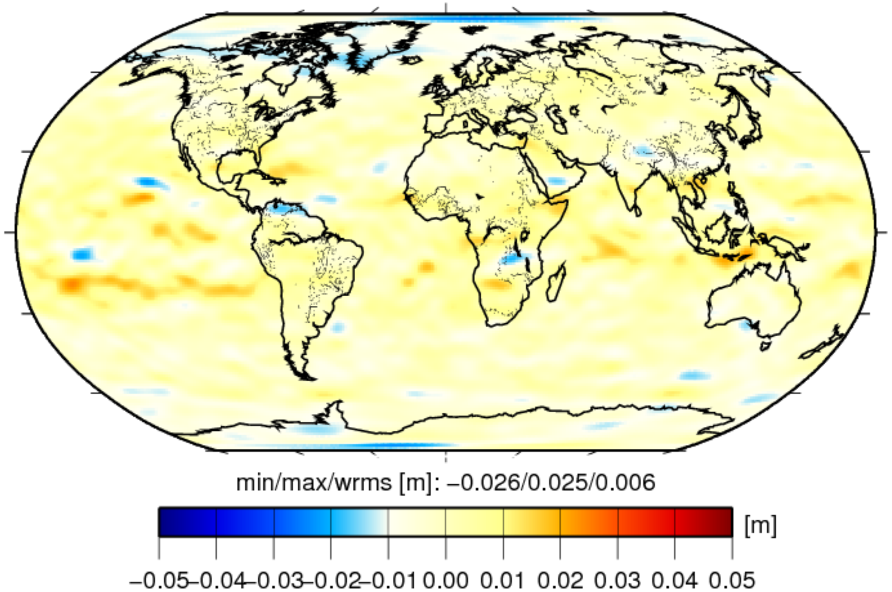

(Differences wrt GOCO05S, 400 km Gauss smoothing adopted)

Systematic signatures along the geomagnetic equator are not visible when using original L1B RINEX GPS data files from the GRACE mission.

(Jäggi et al., 2016)

Data Gaps in RINEX Files

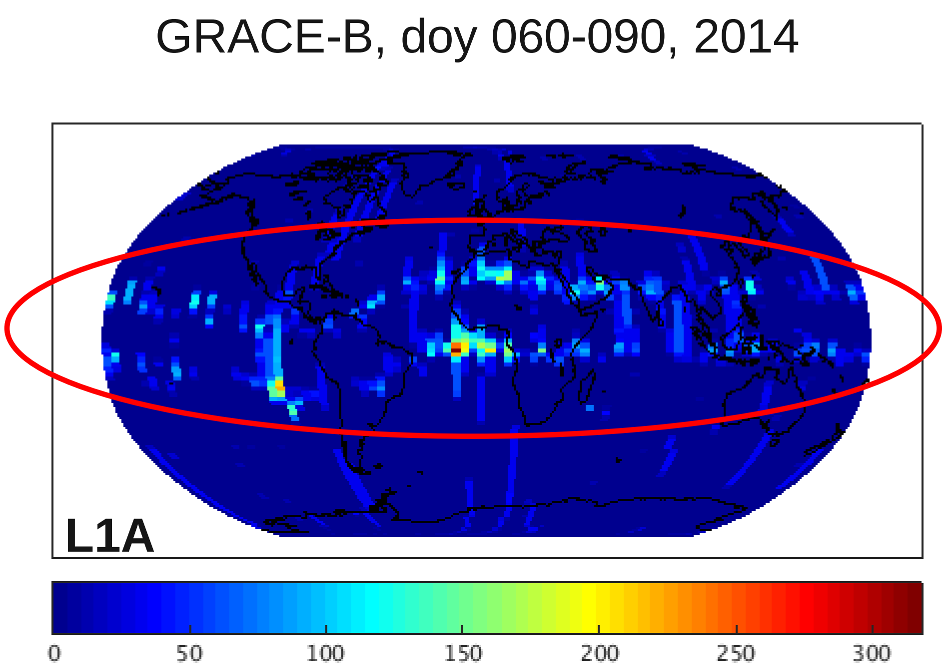

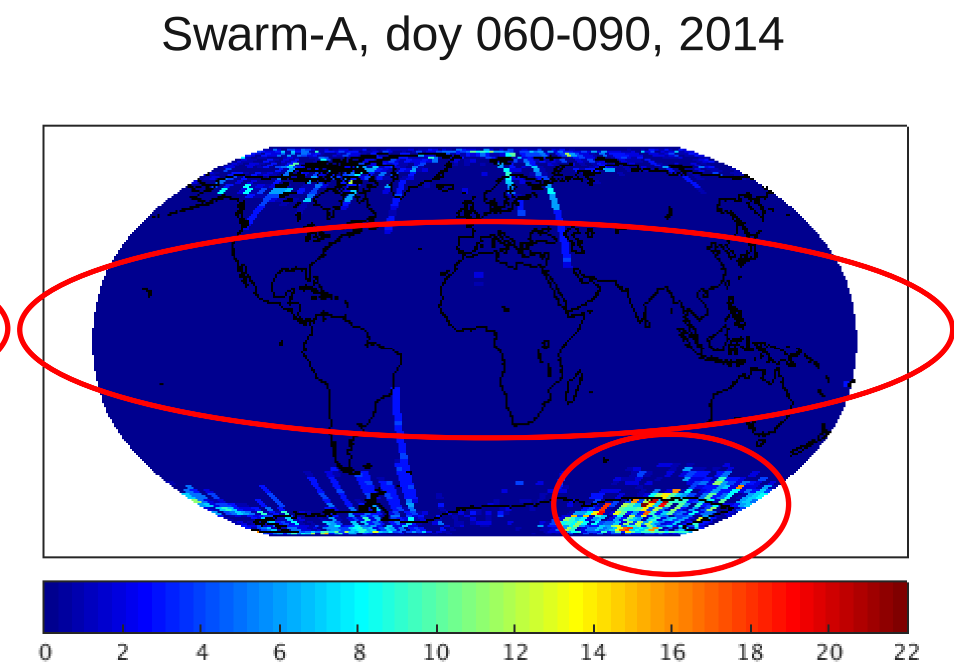

Significant amounts of data are missing in GRACE L1B RINEX files
=> problematic signatures cannot propagate into gravity field.

Swarm RINEX files are more complete (gaps only over the poles)
=> problematic signatures do propagate into the gravity field.

(Jäggi et al., 2016)

Validation Concepts by Satellite Laser Ranging (SLR)

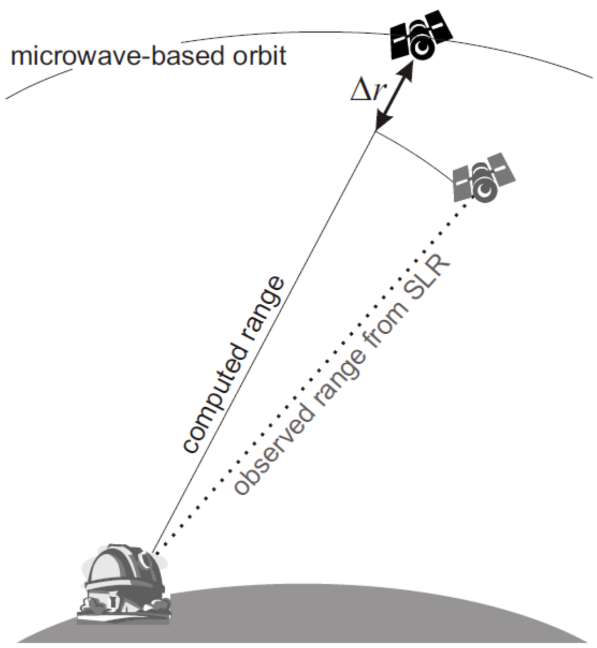

(Flohrer, 2008)

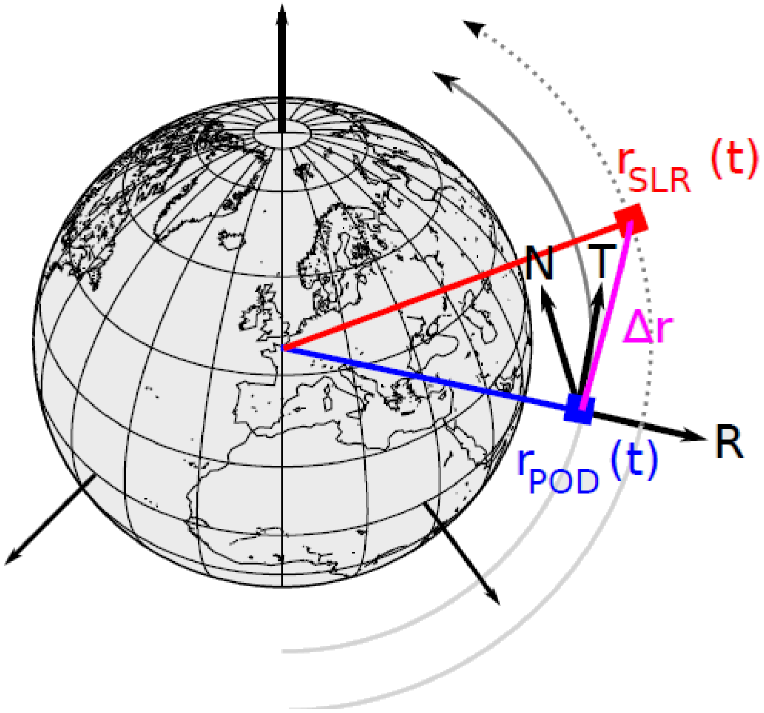

(Hackel et al., 2017)

Examples of SLR Stations in Europe

(Ploner et al., 2015)

© GFZ

Left: **Monostatic** telescope (1-m) of the SLR station in Zimmerwald, Switzerland
Right: **Bistatic** Telescopes (15-/40-cm) of the SLR station in Potsdam, Germany

Examples of SLR Stations in Europe

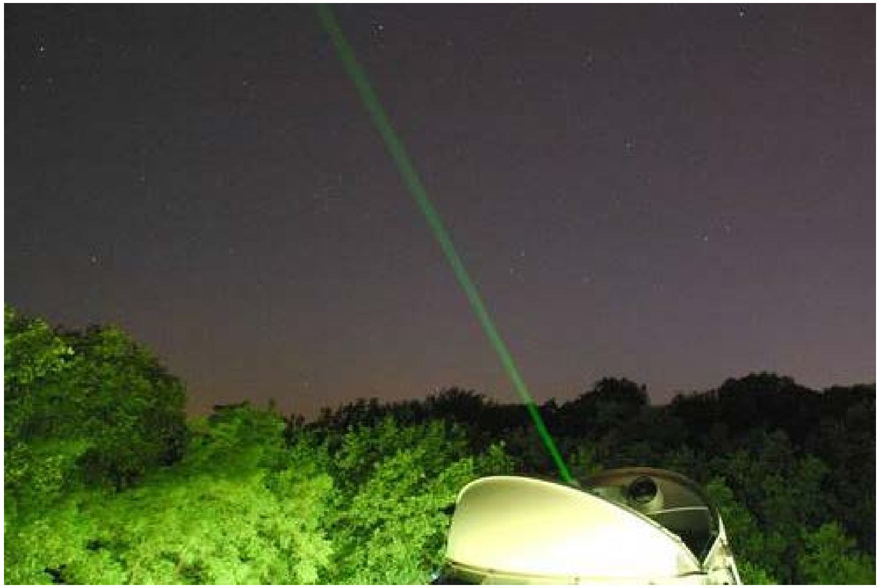

Potsdam:

- Deddicated system for SLR
- 2‘000 Hz Nd:YAG SLR system
- Pulse length: 10 ps, energy: 0.4 mJ

ILRS Station Performance

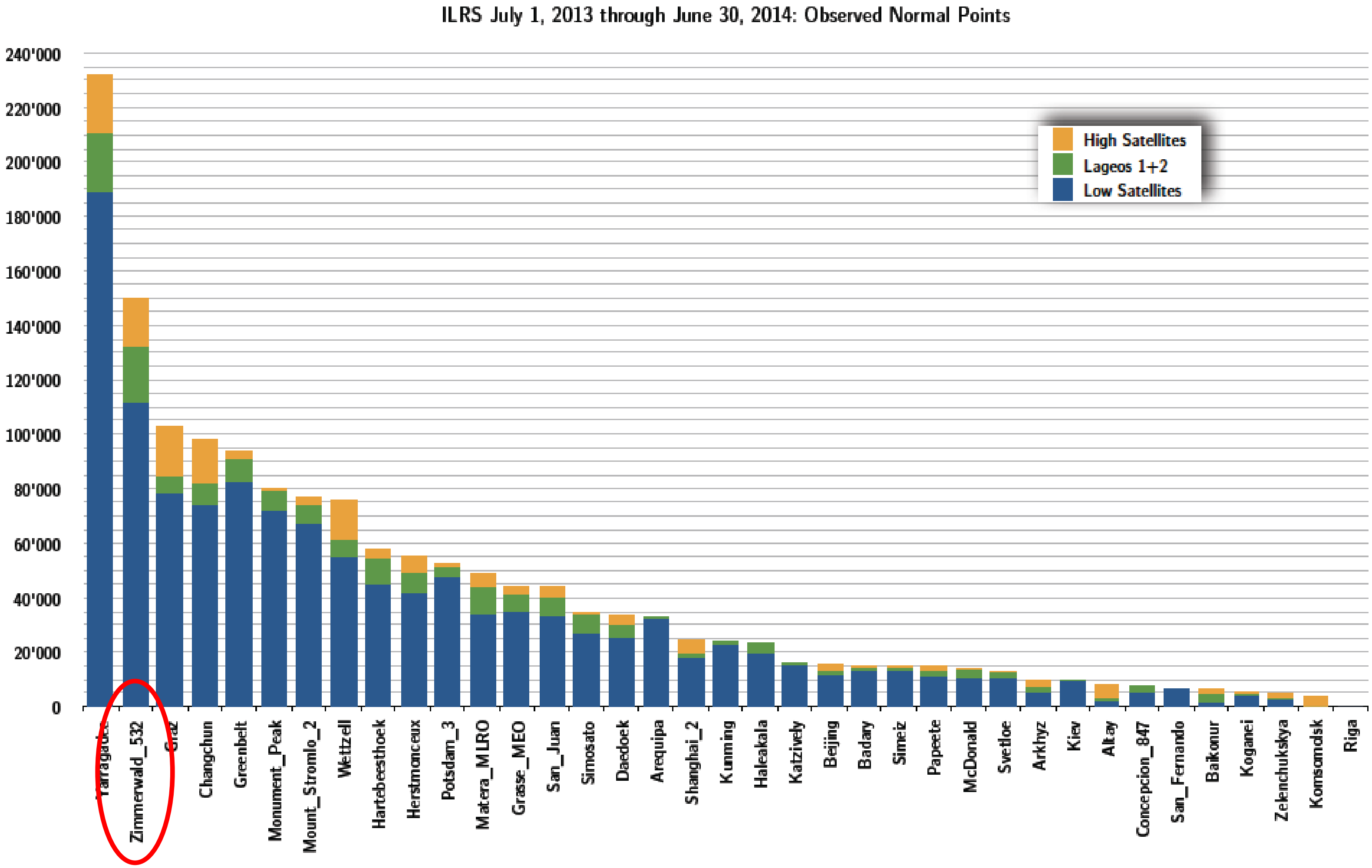

Classical SLR Orbit Validation (GOCE)

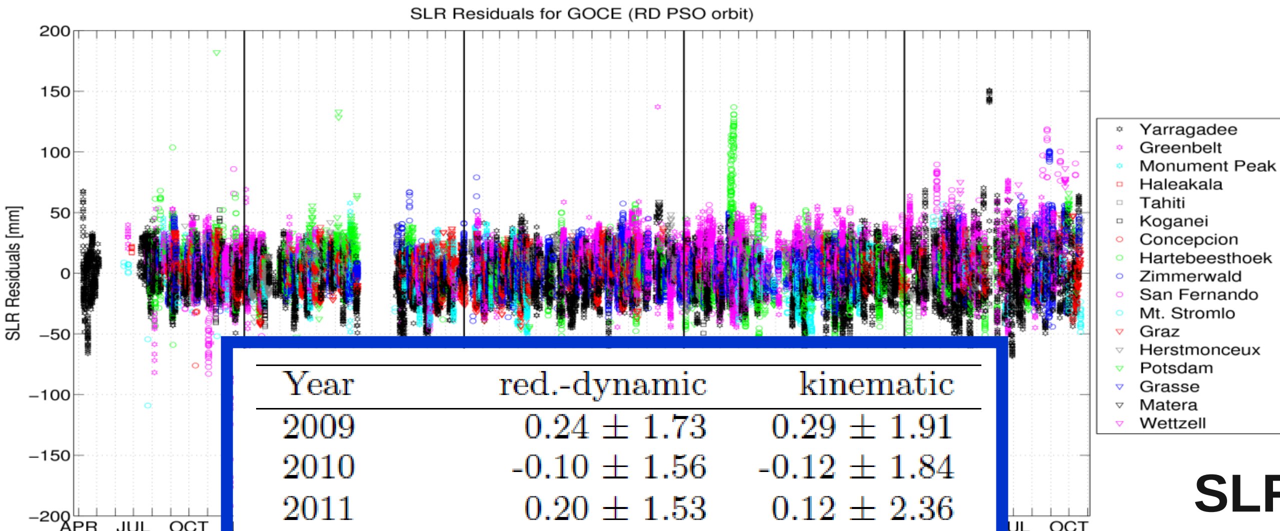

Reduced-dynamic

Year	red.-dynamic	kinematic
2009	0.24 ± 1.73	0.29 ± 1.91
2010	-0.10 ± 1.56	-0.12 ± 1.84
2011	0.20 ± 1.53	0.12 ± 2.36
2012	0.10 ± 1.94	-0.05 ± 2.78
2013	0.63 ± 2.62	0.45 ± 3.17
2009–2013	0.18 ± 1.84	0.10 ± 2.42

SLR statistics:

Mean ± RMS (cm)

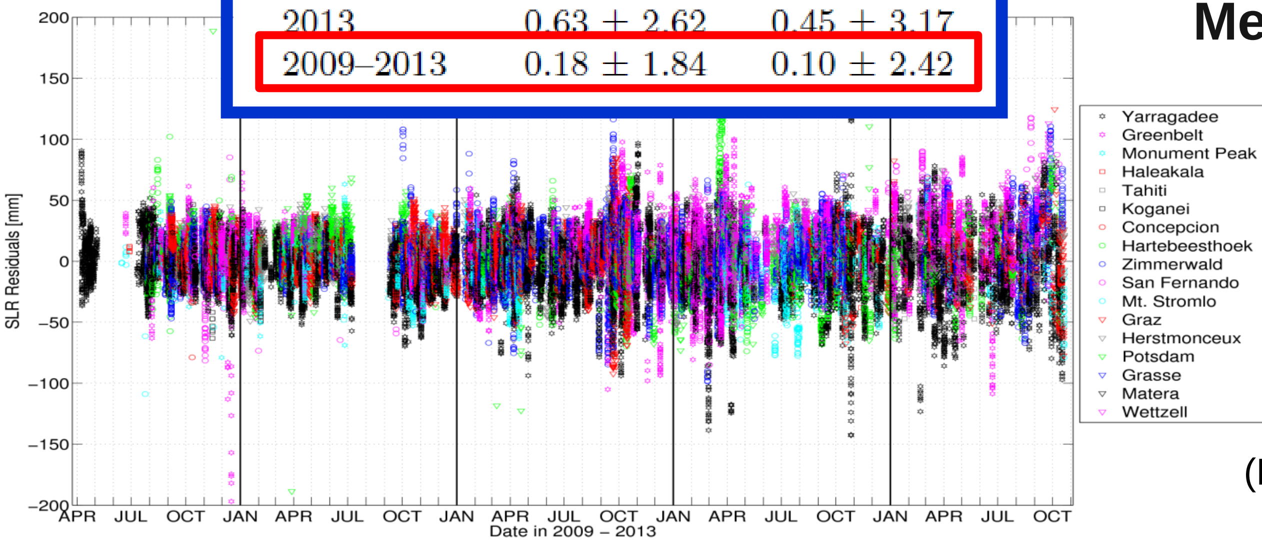

Kinematic

(Bock et al., 2014)

Classical SLR Orbit Validation (Sentinel-3A)

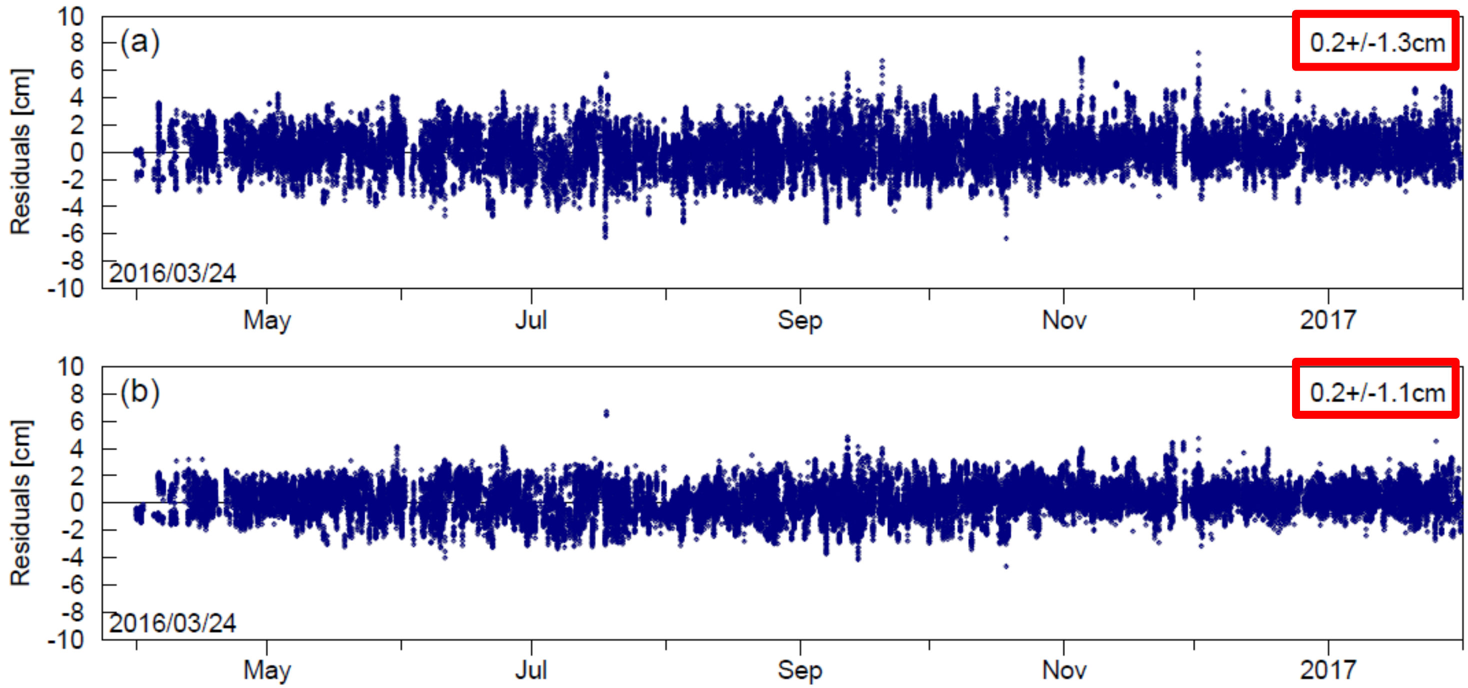

Ambiguity-float solution

Ambiguity-fixed solution

Ambiguity-resolution is not only a key for differential baseline determination (not shown in this lecture), but also for classical POD using undifferenced GPS data.

(Montenbruck et al., 2017)

Different Quality of SLR Stations

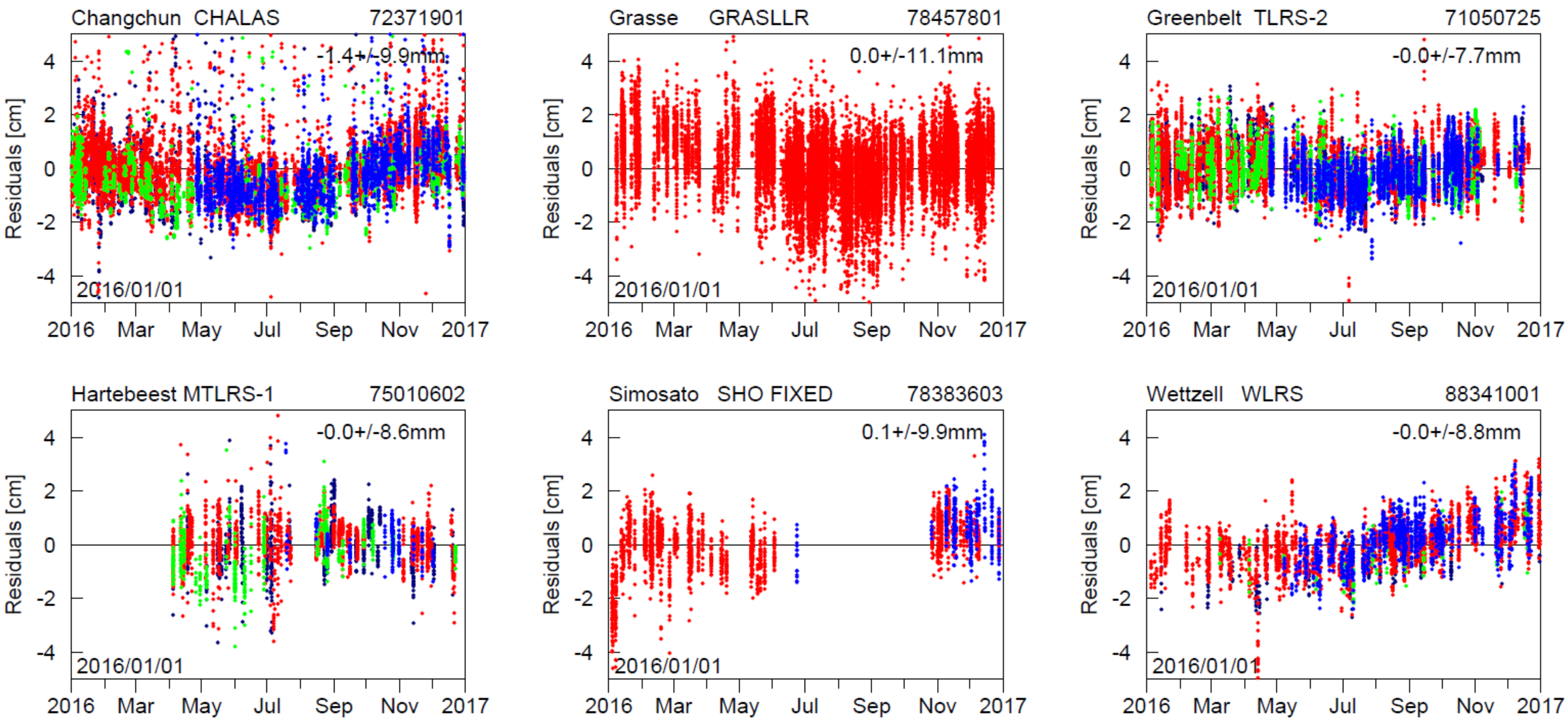

The quality of SLR data differs significantly for different stations. Corrections are needed to use the data from all stations.

(Arnold et al., 2017)

Different Quality of SLR Stations

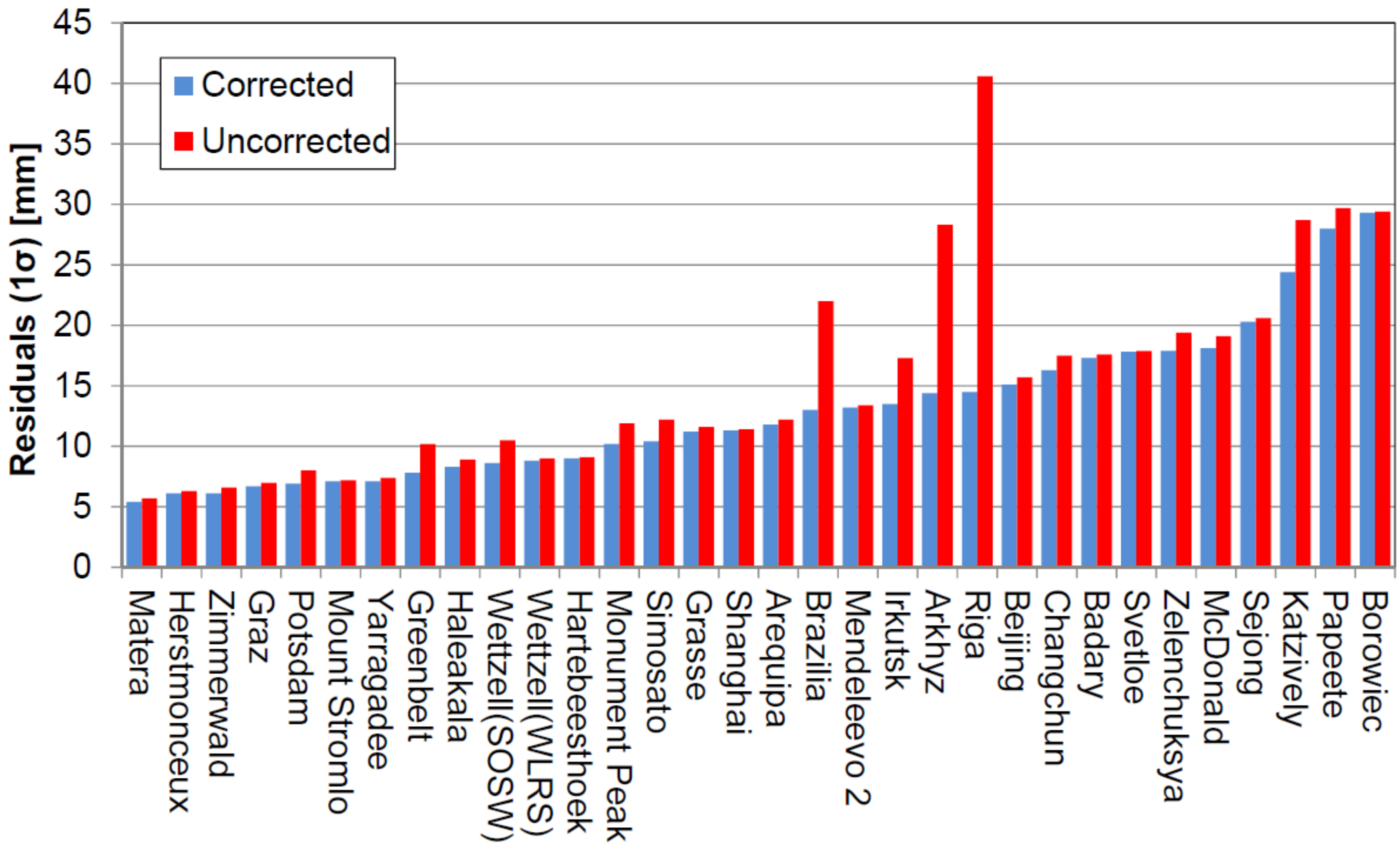

(Arnold et al., 2017)

Subtleties in Modeling SLR Range Data

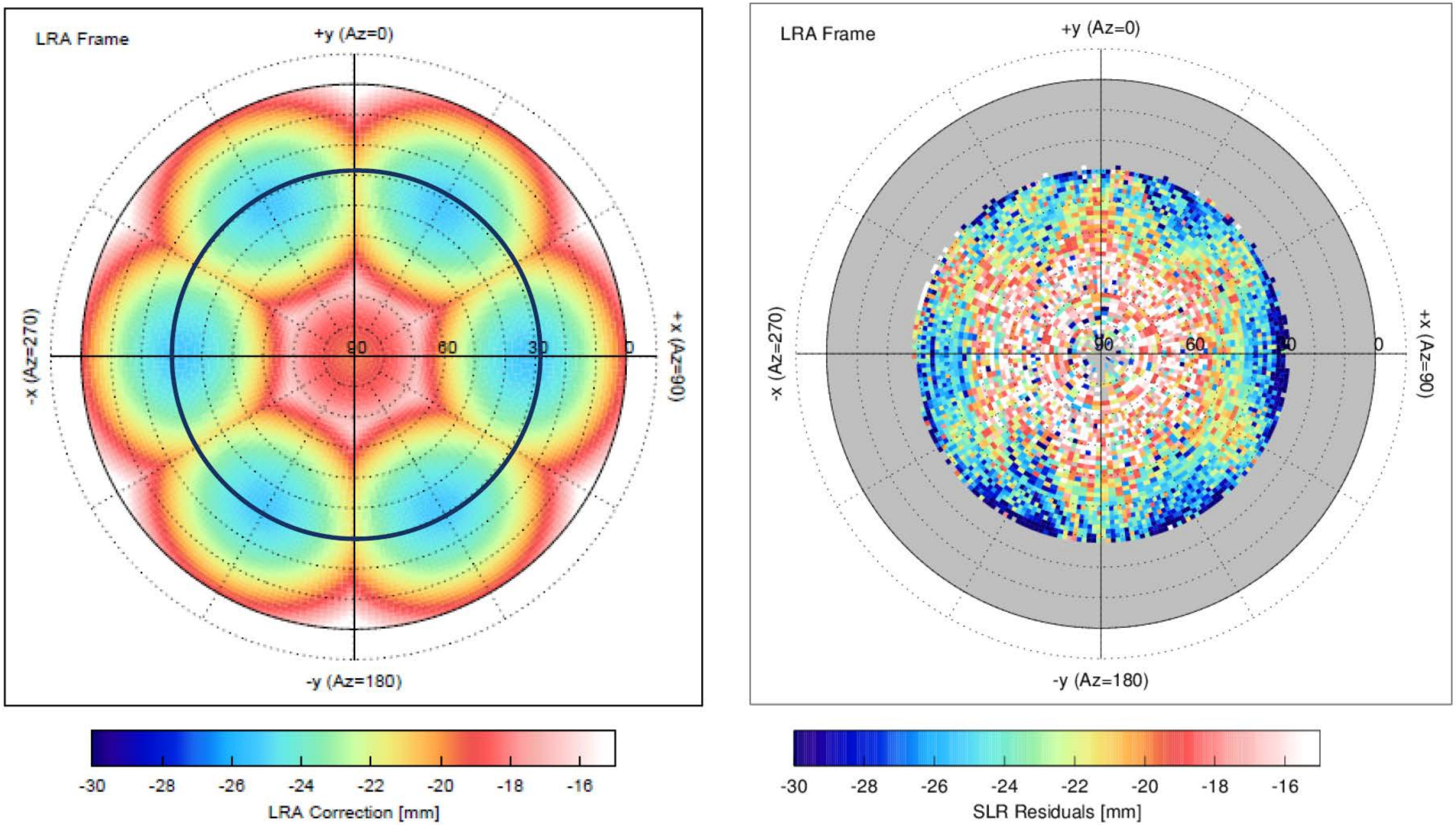

(Arnold et al., 2017)

State-of-the-Art SLR Validation

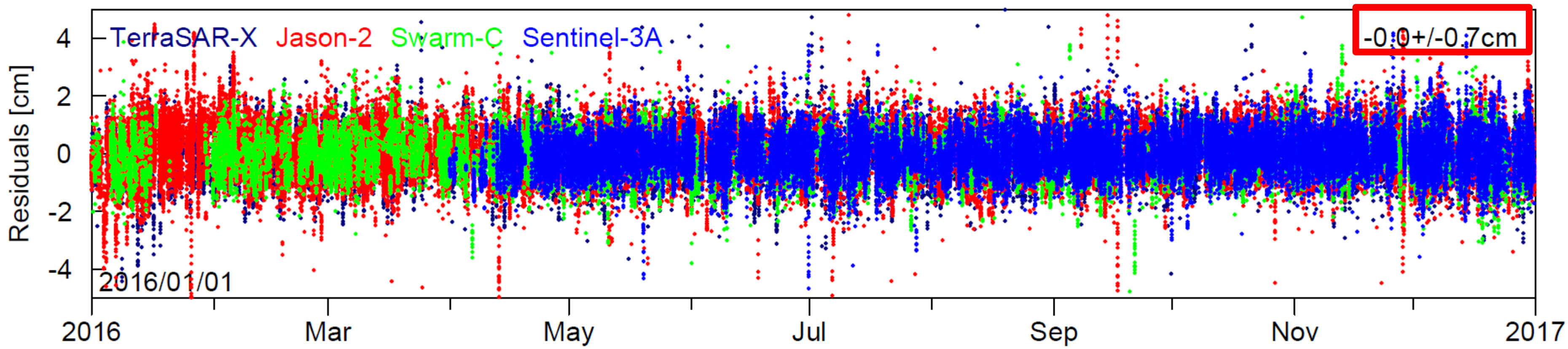

Lessons learnt for LEO SLR validation:

- New reference frame SLRF2014 reduces issues in SLR data. However, selected stations are still suffering from bad coordinates and range biases.

- Systematic orbit and station errors affect the modeled SLR range and need to be separated in long-term analyses for a proper assessment of the orbit quality of state-of-the-art (ambiguity-fixed) precise orbits.

(Arnold et al., 2017)

Time-Variable Gravity Field from Kinematic Positions

Amazon Greenland

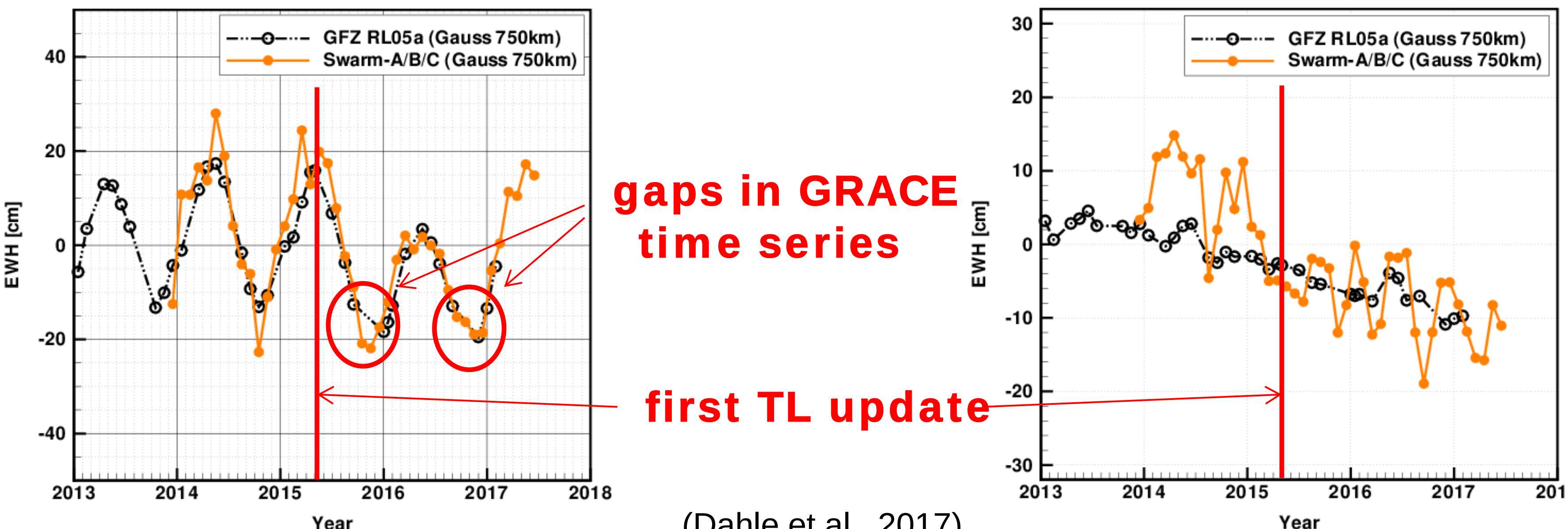

(Dahle et al., 2017)

- Kinematic positions may be used to recover the **long wavelength part** of the Earth's gravity field, including the most pronounced time-variable signal.

- This will be needed to bridge the gap between the dedicated GRACE and GRACE-FO missions. One single mission is, however, not sufficient.

Time-Variable Gravity Field from Kinematic Positions

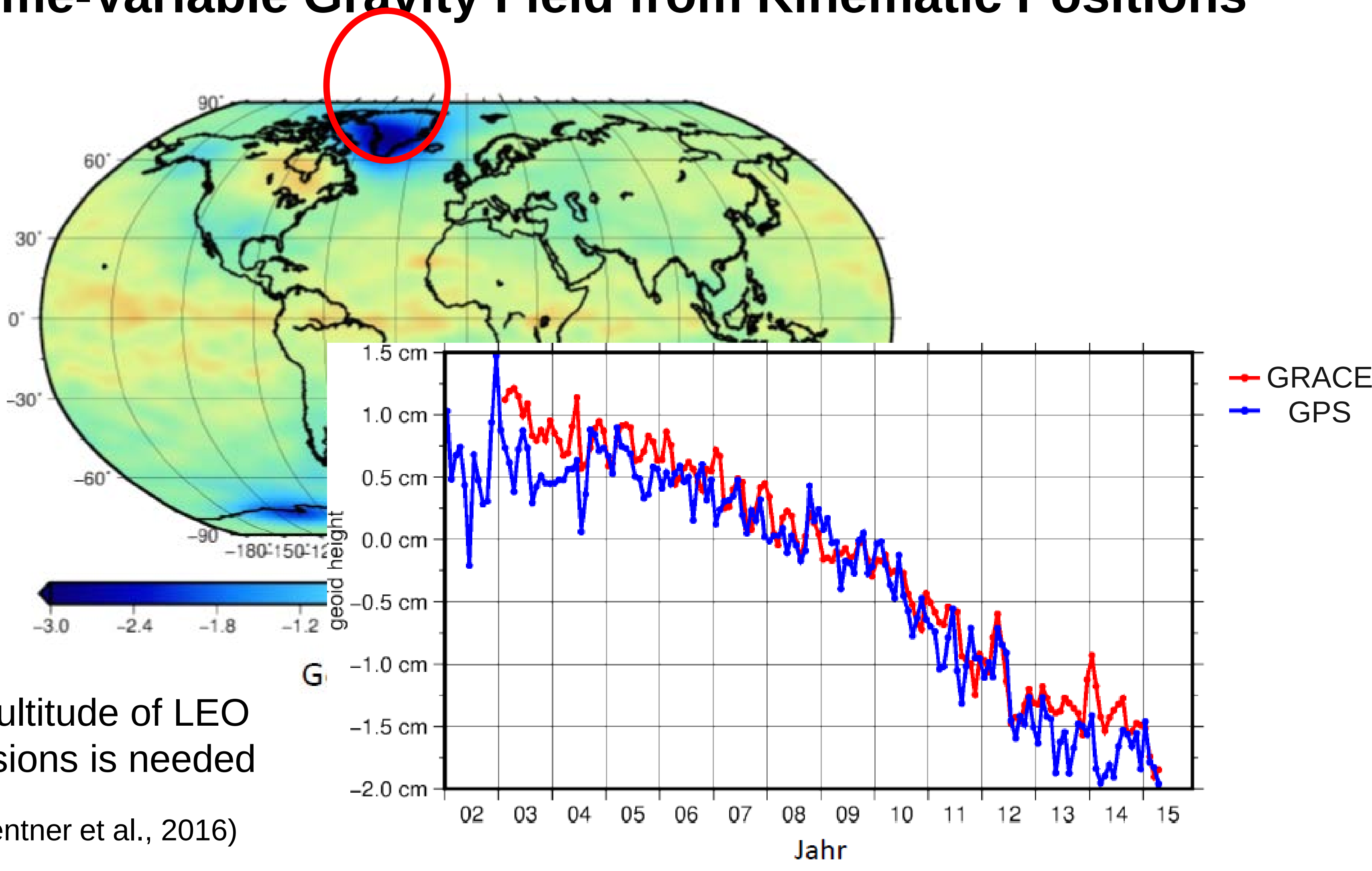

A multitude of LEO missions is needed

(Zehentner et al., 2016)

Time-Variable Gravity Field from Non-Dedicated Data

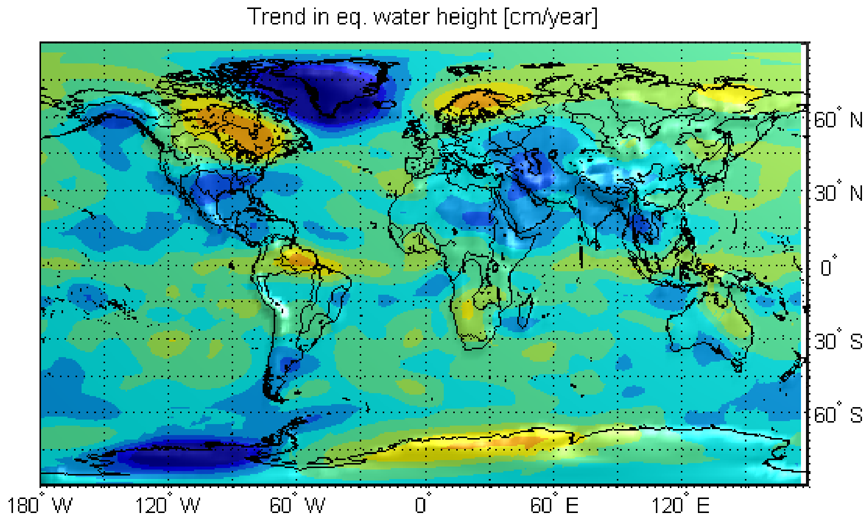

Kin. Pos.

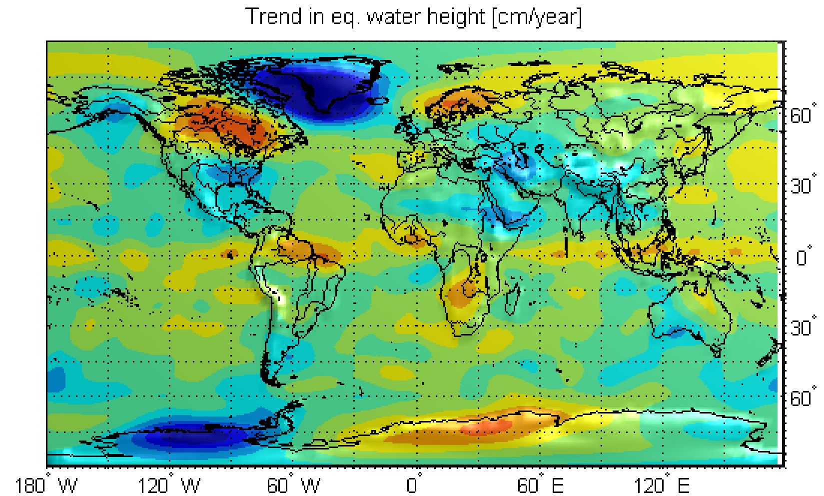

SLR + Kin. Pos.

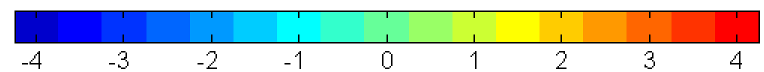

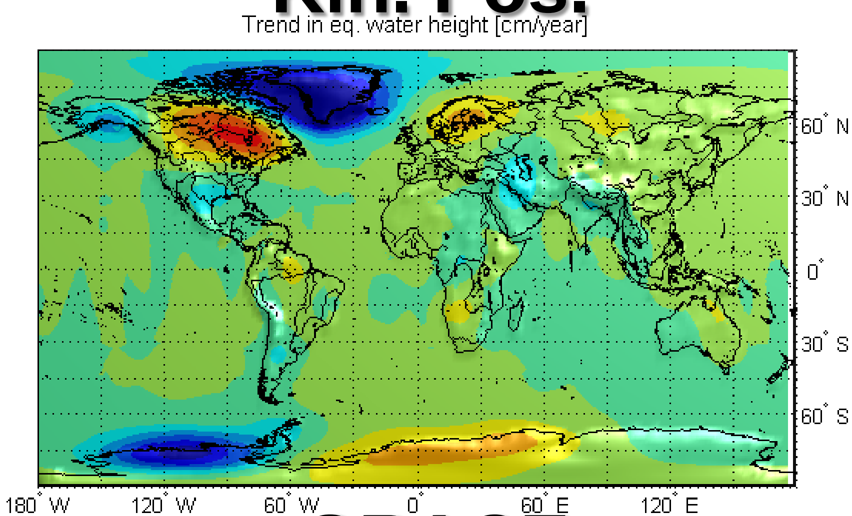

GRACE

Combination of kinematic position solutions with SLR further reduces spurious signals and will be used to bridge the (hopefully small) gap between GRACE and GRACE-FO.

Thank you for your attention

Literature (1)

Arnold, D., M. Meindl, G. Beutler, R. Dach, S. Schaer, S. Lutz, L. Prange, K. Sośnica, L. Mervart, A. Jäggi (2015): CODE's new solar radiation pressure model for GNSS orbit determination. *Journal of Geodesy*, 89(8), 775-791, doi:10.1007/s00190-015-0814-4

Arnold, D., O. Montenbruck, S. Hackel, K. Sośnica (2017): Satellite Laser Ranging to Low Earth Orbiters – Orbit and Network Validation. *Journal of Geodesy*, in preparation

Beutler, G. (2005) Methods of Celestial Mechanics. Vol 1: Physical, Mathematical, and Numerical Principles. Springer, ISBN 3-540-40749-9

Blewitt, G. (1997): Basics of the GPS Technique: Observation Equations, in *Geodetic Applications of GPS*, Swedish Land Survey, pp. 10-54, available at http://www.nbmg.unr.edu/staff/pdfs/blewitt basics of gps.pdf

Bock, H., R. Dach, A. Jäggi, G. Beutler (2009): High-rate GPS clock corrections from CODE: Support of 1 Hz applications. *Journal of Geodesy*, 83(11), 1083-1094, doi:10.1007/s00190-009-0326-1

Bock, H., A. Jäggi, G. Beutler, U. Meyer (2014): GOCE: Precise orbit determination for the entire mission. *Journal of Geodesy*, 88(11), 1047-1060, doi:10.1007/s00190-014-0742-8

Dach, R., E. Brockmann, S. Schaer, G. Beutler, M. Meindl, L. Prange, H. Bock, A. Jäggi, L. Ostini (2009): GNSS processing at CODE: status report. *Journal of Geodesy*, 83(3-4), 353-366, doi:10.1007/s00190-008-0281-2

Literature (2)

Dahle, C., D. Arnold, A. Jäggi (2017): Impact of tracking loop settings of the Swarm GPS receiver on gravity field recovery. *Advances in Space Research*, 59(12), 2843-2854, doi:10.1016/j.asr.2017.03.003

Flohrer, C. (2008): Mutual Validation of Satellite-Geodetic Techniques and its Impact on GNSS Orbit Modeling. *Geodätisch-geophysikalische Arbeiten in der Schweiz*, 75, ISBN 978-3-908440-19-2

Hackel, S., O. Montenbruck, P. Steigenberger, U. Balss, C. Gisinger, M. Eineder (2017): Model improvements and validation of TerraSAR-X precise orbit determination. *Journal of Geodesy*, 91(5), 547-562, doi:10.1007/s00190-016-0982-x

Jäggi, A., H. Bock, R. Pail, H. Goiginger (2008): Highly Reduced Dynamic Orbits and their Use for Global Gravity Field Recovery: A Simulation Study for GOCE. *Studia Geophysica et Geodaetica*, 52(3), 341-359, doi:10.1007/s11200-008-0025-z

Jäggi, A., R. Dach, O. Montenbruck, U. Hugentobler, H. Bock, G. Beutler (2009): Phase center modeling for LEO GPS receiver antennas and its impact on precise orbit determination. *Journal of Geodesy*, 83(12), 1145-1162, doi:10.1007/s00190-009-0333-2

Jäggi, A., H. Bock, U. Meyer, G. Beutler, J. van den IJssel (2015): GOCE: assessment of GPS-only gravity field determination. *Journal of Geodesy*, 89(1), 33-48, doi:10.1007/s00190-014-0759-z

Literature (3)

Jäggi, A., C. Dahle, D. Arnold, H. Bock, U. Meyer, G. Beutler, J. van den IJssel (2016): Swarm kinematic orbits and gravity fields from 18 months of GPS data. *Advances in Space Research*, 57(1), 218-233. doi:10.1016/j.asr.2015/10.035

Jäggi, A., D. Arnold (2017): Precise Orbit Determination. In *Global Gravity Field Modeling from Satellite-to-Satellite Tracking Data*, Lecture Notes in Earth System Sciences, edited by M. Naeimi, J. Flury, pp. 35-80, doi:10.1007/978-3-319-49941-3_2

Montenbruck, O., S. Hackel, A. Jäggi (2017): Precise orbit determination of the Sentinel-3A altimetry satellite using ambiguity-fixed GPS carrier phase observations. *Journal of Geodesy*, submitted

Peter, H., A. Jäggi, J. Fernández, D. Escobar, F. Ayuga, D. Arnold, M. Wermuth, S. Hackel, M. Otten, W. Simons, P. Visser, U. Hugentobler, P. Féménias (2017): Sentinel-1A - First precise orbit determination results. *Advances in Space Research*, 60(5), 879-892, doi:10.1016/j.asr.2017.05.034

Ploner, M., P. Lauber, M. Prohaska, P. Ruzek, T. Schildknecht, A. Jäggi (2015): History of the Laser Observations at Zimmerwald. In *Proceedings of the 19th International Workshop on Laser Ranging*, October 27-31, 2014, Annapolis, Maryland, USA

Sušnik, A., A. Grahsl, D. Arnold, A. Villiger, R. Dach, A. Jäggi (2017): GNSS reprocessing results in the framework of the EGSIEM project. *Journal of Geodesy*, submitted

Literature (4)

Švehla, D., M. Rothacher (2004): Kinematic Precise Orbit Determination for Gravity Field Determination, in *A Window on the Future of Geodesy*, edited by F. Sanso, pp. 181-188, Springer, doi:10.1007/b139065

Teunissen, P.J.G., O. Montenbruck (Eds.) (2017): Springer Handbook of Global Navigation Satellite Systems, ISBN 978-3-319-42928-1

Zehentner, N., T. Mayer-Gürr (2016): Precise Orbit Determinaton Based on Raw GPS Measurements, *Journal of Geodesy*, 90(3), 275-286, doi:10.1007/s00190-015-0872-7